performed comparative targeted proteomic analysis of the lipid droplet proteins in HCV core–expressing and non-expressing hepatoma cell lines using two strategies: conventional 1-D-SDS-PAGE/MALDI-TOF mass spectrometry (MS) and automated high-throughput direct nanoflow liquid chromatography (DNLC)–MS/MS. We found prominent differences in the protein compositions of lipid droplets between HCV core–expressing and non-expressing hepatoma cell lines.

MATERIALS AND METHODS

Cell Lines—The human hepatoma HepG2 cell line constitutively expressing HCV core protein (Hep39) was established as described previously (*47*). Another HepG2 cell line transfected with expression vector pcEF321swxneo without the HCV core protein insert (Hepswx) was used as a mock control (*47*). Both cell lines were plated on collagen-coated dishes (Asahi Techno Glass, Tokyo, Japan) and maintained in the normal culture medium [DMEM supplemented with 10% fetal bovine serum, 100 units/ml Penicillin G, 100 μg/ml streptomycin sulfate, and 1 mg/ml G418 (Sigma, St. Louis, MO, USA)] under a 5% CO_2 atmosphere at 37°C.

Lipid Droplet Preparation—Hepswx and Hep39 cells were seeded at 4×10^6 cells/dish (150 mm, inner diameter) in 25 ml of normal culture medium and cultured for one day. For efficient formation of lipid droplets by cells, cholesterol (final 20 μg/ml) and oleic acid (final 400 μM)/fatty acid–free BSA (final 60 μM) complex, prepared as stock solutions of 5 mg/ml cholesterol in ethanol and 10 mM oleic acid/1.5 mM BSA in PBS, respectively, were added to the medium. Each cell line was further incubated for 48–72 h at 37°C. For proteomic analysis of lipid droplet proteins, confluent monolayers of Hepswx and Hep39 cells in fifteen cell culture dishes (150 mm, inner diameter) were harvested by scraping and pelleted by centrifugation ($200 \times g$ for 5 min at 4°C). After being washed with PBS three times, each cell pellet was resuspended in 10 mM Tris-HCl buffer, pH 7.5, containing 0.25 M sucrose and Complete™, EDTA-free (Roche, Mannheim, Germany) to achieve a final volume equal to five times the volume of the cell pellet (*i.e.* a 20% cell suspension). The cell suspension was homogenized with a ball-bearing homogenizer (*48*), and then centrifuged at $800 \times g$ for 5 min at 4°C. One milliliter of each post-nuclear supernatant fraction was layered under 2 ml of 10 mM Tris-HCl buffer, pH 7.5, containing 0.15 M NaCl (TN-buffer). After centrifugation at $100{,}000 \times g$ for 60 min at 4°C, the lipid droplet fraction, *i.e.* the distinct white band on the top of the preparation, was collected with a pipetman. The floating lipid droplet fraction was diluted with 3.5 ml of TN-buffer and then re-purified by centrifugation ($100{,}000 \times g$ for 30 min at 4°C). This washing step was repeated three times. Lipid droplets in the floating fractions in both cells were enriched up to more than 500-fold compared with those in the total cell lysates as estimated by their protein contents. The amounts of lipid droplets isolated from Hepswx and Hep39 cells were nearly the same. The purified lipid droplet fractions (~0.1 mg of protein per ml) were stored at −80°C until use. The purity of the lipid droplet fractions was verified by microscopic and immunoblot (Fig. 1) analyses. Adipose differentiation–related protein (ADRP), a known lipid droplet protein, was significantly enriched in the lipid droplet fractions of Hepswx and Hep39 cells (Fig. 1). Other organelle marker proteins, such as nucleoporin p62 for the nucleus, prohibitin for the mitochondria, fatty acid synthase for the cytoplasm, GM130 for the Golgi apparatus, EEA1 for the early endosome, or annexin II for the plasma membrane, were not detected in the lipid droplet fractions of either cells (Fig. 1). Small amounts of calnexin, a marker of the endoplasmic reticulum, which is a major organelle, were detected in the lipid droplet fractions of both cells to a similar extent. Although we did not detect calnexin in the lipid droplet fractions by proteomic analysis (see Tables 1 and 2), the lipid droplet fractions of both cells could be contaminated with a small amount of endoplasmic reticulum.

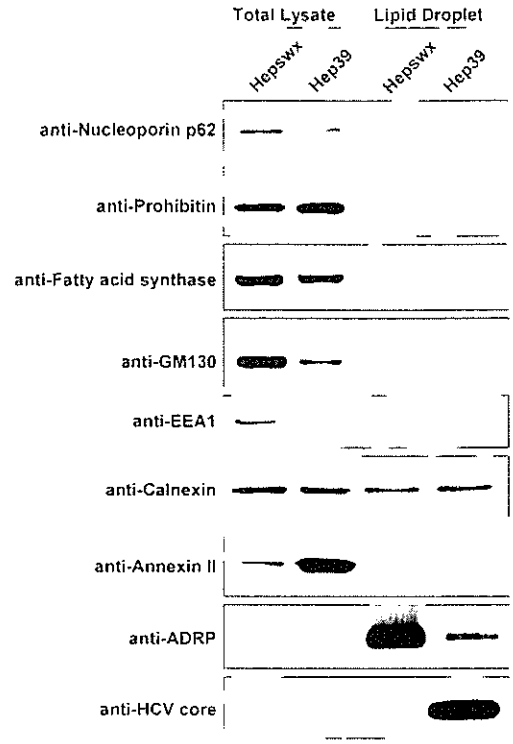

Fig. 1. **Immunoblot analysis of lipid droplet fractions in Hepswx and Hep39 cells using antibodies against various organelle markers.** Total cell lysates and lipid droplet fractions (1.5 μg of protein per lane in the case of anti-ADRP; 5 μg of protein per lane in others) from Hepswx and Hep39 cells were analyzed by immunoblotting with the indicated antibodies.

1-D-SDS-PAGE/MALDI-TOF MS Analysis—The lipid droplet fraction (30 μg protein) of each cell line was fractionated in a 10% SDS–polyacrylamide gel, and the gel was stained with Coomassie Brilliant Blue. The protein bands were excised from the gel and subjected to in-gel trypsin digestion. The tryptic peptide mixtures were analyzed by MALDI-TOF MS as described previously (*49*). Prior to MALDI-TOF MS analysis, the peptide mixtures were desalted using C18 Zip Tips (Millipore, Billerica, MA, USA) according to the manufacturer's instructions. The peptide data were collected in the reflection mode and with positive polarity, using a saturated solution of

Table 1. **Lipid droplet proteins identified in Hepswx and Hep39 cells by means of 1-D-SDS-PAGE/MALDI-TOF MS.**

Protein	Molecular mass (kDa) (calc.)	Accession No.	SDS band No.[a]	
			Hepswx	Hep39
PAT family proteins				
Adipose differentiation–related protein (ADRP)	48.1	34577059	5	21
Cargo selection protein/TIP47	47.0	20127486		22
Lipid metabolism				
Acyl CoA synthetase long chain family member 3	80.4	42794752	4	18
Cytochrome b_5 reductase	34.3	4503327	9	26
Lanosterol synthase	83.3	4808278	4	18
NAD(P)-dependent steroid dehydrogenase-like; H105e3	41.9	8393516	8	25
Retinal short-chain dehydrogenase/reductase retSDR2	33.0	7705905	10	27
Cytosolic phospholipase A_2	85.2	1352707		14
Rab GTPases				
Rab1A	22.7	4758988	13	30
Rab1B	22.2	23396834	13	30
Rab5C	23.5	38258923	11	28
Rab7	23.5	34147513	12	29
RNA metabolism/binding				
DEAD box protein 1 (DDX1)	82.9	6919862		16
DEAD box protein 3 (DDX3)	73.2	3023628		18
HC56/gemin 4	118.8	10945430		15
Other/unknown proteins				
BiP protein	70.9	14916999	3	17
CGI-49 protein	46.9	7705767	6	23
Heat shock protein gp96 precursor	90.2	15010550	2	14
Ancient ubiquitous protein 1	41.4	31712024	7	
Major vault protein	99.3	15990478	1	
Apoptosis-inducing factor–homologous mitochondrion-associated inducer of death	40.5	13543964		24
KIAA0887 protein	52.4	4240263		21
Protein disulfide-isomerase [EC 5.3.4.1] ER60 precursor	56.7	1085373		20
Transport-secretion protein 2.1	57.7	9663151		19
HCV core protein	20.6	974345		31

[a]Band numbers correspond to those in Fig. 2.

α-cyano-4-hydroxycinnamic acid (Sigma) in 50% acetonitrile and 0.1% trifluoroacetic acid as the matrix. Spectra were obtained using a Voyager DE-STR MALDI-TOF mass spectrometer (PE Biosystems, Foster City, CA, USA). Internal calibration was performed with adrenocorticotropic hormone, fragment 18–39 (Sigma), and bradykinin fragment (Sigma). The data base–fitting program MS-Fit available at the WWW site of the University of California, San Francisco (prospector.ucsf.edu/ucsfhtml3.4/msfit.htm) was used to interpret the MS spectra of protein digests (*50*).

DNLC-MS/MS Analysis—The lipid droplet fraction (10 μg protein) of each cell line was first delipidated by chloroform–methanol extraction as originally described (*51*). Two volumes of chloroform and 1 volume of methanol were mixed with 0.8 volume of the lipid droplet fraction. Then, 1 volume of chloroform and 1 volume of water were added to the mixture, and the mixture was vortexed for 30 s, and centrifuged at 10,000 × *g* for 5 min at room temperature. The resulting organic (lower) phase was removed. The aqueous (upper) phase and interface, containing all the lipid droplet proteins, was lyophilized. The delipidated lipid droplet proteins were digested with endoproteinase Lys-C, and the resulting peptides were analyzed by DNLC-MS/MS as described (*52*, *53*).

Cell Fractionation—All manipulations were performed at 4°C or on ice. After being washed with PBS, confluent monolayers of Hepswx and Hep39 cells were harvested by scraping and pelleted by centrifugation (200 × *g*, 5 min). The precipitated cells were homogenized with a ball-bearing homogenizer in 10 mM Tris-HCl buffer, pH 7.5, containing 0.25 M sucrose, and Complete™, EDTA-free. After centrifugation of the lysate at 800 × *g* for 5 min, the cytosolic fraction (100,000 × *g* supernatant) and membrane fraction (100,000 × *g* precipitate) were separated from the post-nuclear supernatant fraction by centrifugation at 100,000 × *g* for 60 min. The membrane fraction was resuspended in TN-buffer and then re-purified twice by centrifugation. The protein concentrations of these preparations were determined with BCA protein assay reagents (Pierce Biotechnology, Rockford, IL, USA) using BSA as a standard.

Immunoblot Analysis—Equivalent amounts of proteins from Hepswx and Hep39 cells were separated in a 10 or 12.5% SDS–polyacrylamide gel and then electrophoretically transferred to a polyvinylidene difluoride membrane. The membranes were blocked overnight at 4°C or 30 min at room temperature in TBS containing 0.1% Tween 20 and 5% skim milk. The blots were probed with a mouse

Table 2. **Lipid droplet proteins identified in Hepswx and Hep39 cells by means of DNLC-MS/MS.**

Protein	Accession No.	Molecular mass (kDa) (calc.)	Matched peptide sequence	
			Hepswx[a]	Hep39[a]
PAT family proteins				
Adipose differentiation–related protein (ADRP)	34577059	48.1	+ TITSVAMTSALPIIQK DAVTTTVTGAK EVSDSLLTSSK	+ TITSVAMTSALPIIQK DAVTTTVTGAK EVSDSLLTSSK
Cargo selection protein / TIP47	20127486	47.0	+ VSGAQEMVSSAK	+ VSGAQEMVSSAK
Lipid metabolism				
Acyl-CoA synthetase long-chain family member 3	42794752	80.4	+ VLSEAAISASLEK	+ ELTELARK
Cytochrome b_5 reductase	4503327	34.2	+ DILLRPELEELRNK	+ SNPIIRTVK
Gastric-associated differentially-expressed protein YA61P	6970062	14.9	+ AIGLVVPSLTGK	+ AIGLVVPSLTGK
Retinal short-chain dehydrogenase/ reductase retSDR2	7705905	33.0	+ HGLEETAAK	+ FDAVIGYK
Sterol carrier protein 2–related form, 58.85K	86717	58.8	+ LQNLQLQPGNAK	+ LQNLQLQPGNAK
Acyl-CoA synthetase long-chain family member 4	4758332	74.4	+ SDQSYVISFVVPNQK	
Fatty acid binding protein 5	4557581	15.2	+ ELGVGIALRK	
Hydroxysteroid (17-beta) dehydrogenase 4	4504505	79.7		+ NHPMTPEAVK
Rab GTPases				
Rab1A	4758988	22.6	+[b] QWLQEIDRYASENVNK RMGPGATAGGAEK	+ RMGPGATAGGAEK
Rab1B	23396834	22.1	+[b] QWLQEIDRYASENVNK	+ RMGPGAASGGERPNLK
Rab7	34147513	23.5	+ NNIPYFETSAK	+ ATIGADFLTK
Rab18	20809384	22.9	+ HSMLFIEASAK	+ ILIIGESGVGK
Rab10	12654157	22.5	+ LLLIGDSGVGK	
Rab11	4758986	24.5	+ VVLIGDSGVGK	
Rab8	539607	23.6		+ IRTIELDGK
RNA metabolism/binding				
DEAD box protein 1 (DDX1)	6919862	82.4		+ FGFGFGGTGK
DEAD box protein 3 (DDX3)	3023628	73.2		+ GVRHTMMFSATFPK
IGF-II mRNA-binding protein 3	30795212	63.7		+ EGATIRNITK
Ribosomal protein L29	14286258	17.8		+ AQAAAPASVPAQAPK
Other/unknown proteins				
Apoptosis-inducing factor homologous mitochondrion-associated inducer of death	13543964	40.5	+ EVTLIHSQVALADK	+ EVTLIHSQVALADK
BiP protein	14916999	72.3	+ SQIFSTASDNQPTVTIK	+ VYEGERPLTK
Hypothetical protein DKFZp586A0522.1	7512845	28.2	+ LQHIQAPLSWELVRPH-IYGYAVK	+ RELFSNLQEFAGPSGK
Prolyl 4-hydroxylase, beta subunit	20070125	57.1	+ VHSFPTLK	+ AEGSEIRLAK
Ancient ubiquitous protein 1	31712024	41.4	+ GTQSLPTASASK	
Heat shock protein gp96 precursor	15010550	90.2	+ FAFQAEVNRMMK	
Hypothetical protein FLJ21820	11345458	37.3	+ DIYGLNGQIEHK	
Molecule possessing ankyrin repeats induced by lipopolysaccharide	38173790	78.1	+ CLIQMGAAVEAK	
Ubiquitin-conjugating enzyme E2G 2, isoform 1	15079469	18.6	+ RLMAEYK	
CGI-49 protein	7705767	46.9		+ AGGVFTPGAAFSK
DILV594	37182139	31.4		+ RELFSQIK
Hypothetical protein DKFZp564F0522.1—human (fragment)	7512734	33.1		+ ILRTSSGSIREK
Hypothetical protein HSPC117	7657015	55.2		+ EQLAQAMFDHIPVGVGSK
Tumor protein D52–like 2 isoform e	40805860	22.2		+ TQETLSQAGQK
Vesicle amine transport protein 1	15679945	41.9		+ VVTYGMANLLTGPK

[a]+, detected. [b]This peptide sequence is present in both Rab1A and Rab1B.

monoclonal anti-ADRP antibody (PROGEN Biotechnik GmbH, Heidelberg, Germany) (1:25), a guinea pig polyclonal anti-TIP47 antibody (PROGEN Biotechnik GmbH) (1:250), a mouse monoclonal anti-HCV core protein antibody (Anogen, Ontario, Canada) (1: 1,000), a mouse monoclonal anti-DDX1 antibody (Pharmingen, San Diego, CA, USA) (1:500), or a rabbit polyclonal anti-DDX3 antibody (antibody custom-made by Invitrogen, CA, USA) (1:500) for 90 min at room temperature. The blots were then incubated with horseradish peroxidase (HRP)–conjugated goat anti-rabbit IgG (BIO-RAD), HRP-conjugated goat anti-mouse IgG (BIO-RAD), or HRP-conjugated goat anti-guinea pig IgG (ICN Pharmaceuticals, Aurora, OH, USA) at 1:2,000 dilution for 60 min. Detection of immunoreactive proteins was performed with an ECL system (Amersham Biosciences Corp., Piscataway, NJ, USA).

RESULTS

Proteomic Analysis of Lipid Droplets by 1-D-SDS-PAGE/MALDI-TOF MS—Lipid droplet proteins from control (HCV core non-expressing) Hepswx cells and HCV core–expressing Hep39 cells were separated by 10% SDS-PAGE, and the protein bands were visualized by Coomassie Brilliant Blue staining (Fig. 2). In each cell line ~30 bands were seen. The visible bands (areas) were excised from the gels, trypsinized, and analyzed by MALDI-TOF MS. Among the 31 bands, we identified 25 proteins: 15 proteins in Hepswx cells and 23 proteins in Hep39 cells (Fig. 2 and Table 1). Thirteen of the 25 proteins were detected in both types of cell. The lipid droplet proteins found in both Hepswx and Hep39 cells could be categorized into four groups: (1) PAT family proteins, *i.e.* ADRP and TIP47; (2) multiple molecules involved in lipid metabolism; (3) several Rab GTPases; and (4) other/unknown proteins (Table 1). In addition, Hep39 cells contained another group of proteins involved in RNA metabolism/binding (Table 1).

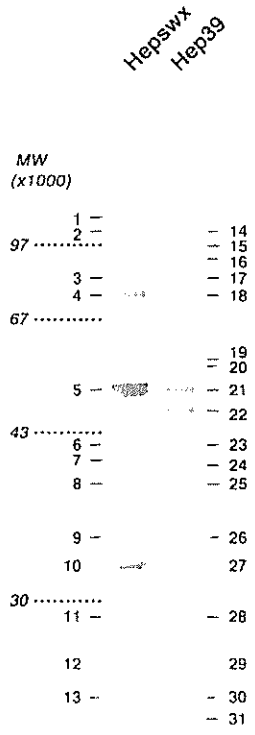

Fig. 2. **Signature SDS-PAGE patterns of the lipid droplet fractions of Hepswx and Hep39 cells.** Proteins in the purified lipid droplet fractions (30 μg of protein per lane) of Hepswx cells and Hep39 cells were separated in a 10% SDS–polyacrylamide gel, and visualized by Coomassie Brilliant Blue staining. The 31 numbered bands were excised from the gel, subjected to in-gel trypsin digestion, and processed for MALDI-TOF-MS. Molecular weights (MW) are given to the left of the gel.

Proteomic Analysis of Lipid Droplets by DNLC-MS/MS—Some protein bands in Fig. 2 could not be identified, probably due to the restricted separation capacity of 1-D-SDS-PAGE (*i.e.* multiple proteins migrating to the same area). We had, however, difficulty in applying 2-DE to the separation of lipid droplet proteins because of their hydrophobic characteristics. We then tried a new LC-based MS strategy. Lipid droplet fractions from Hepswx and Hep39 cells were delipidated and then digested with Lys-C. The resulting peptide mixtures were directly analyzed using a DNLC-MS/MS system (*52*). We identified 36 lipid droplet proteins: 24 proteins in Hepswx cells and 27 proteins in Hep39 cells (Table 2). Twenty-three lipid droplet proteins were newly identified with this system. Fifteen proteins detected in both cell lines were classified into four categories (Table 2) as in the case of 1-D-SDS-PAGE/MALDI-TOF MS analysis. A group of proteins involved in RNA metabolism/binding was also found only in Hep39 cells (Table 2).

Proteins Exhibiting Differences in Their Association with Lipid Droplets Due to HCV Core Protein Expression—SDS-PAGE patterns of lipid droplet proteins were similar but revealed several distinct differences in protein composition between Hepswx and Hep39 cells (Fig. 2). The most remarkable differences were seen in the bands corresponding to PAT family proteins. The amount of ADRP, a major PAT family protein in lipid droplets in the liver (*54*, *55*), and likely to be the most abundant lipid droplet protein in Hepswx cells (Fig. 2, band 5), seemed to be less in HCV core–expressing Hep39 cells (Fig. 2, band 21). On the other hand, TIP47, which is also known to be a PAT family protein in lipid droplets (*56*, *57*), was detected as a major protein only in Hep39 cells (Fig. 2, band 22, and Table 1). To confirm these findings, the contents of ADRP and TIP47 in the lipid droplet fractions of Hepswx and Hep39 cells were examined by immunoblot analysis with specific antibodies. The lipid droplet fraction of HCV core–expressing Hep39 cells showed an apparently lower content of ADRP and a much higher content of TIP47 than the levels in Hepswx cells (Fig. 3).

Next we examined the cellular distributions of ADRP and TIP47 in Hepswx and Hep39 cells by cell fractionation. ADRP was highly concentrated in the lipid droplet fractions of both cells, even though the content in the lipid droplets was much lower in Hep39 cells than in Hepswx cells (Fig. 4). ADRP was not detected in post-nuclear supernatant fractions or in either the cytosol or membrane fractions, probably because of low expression levels in these cells or low affinity of the anti-ADRP antibody we used

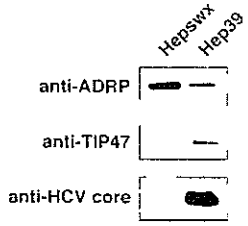

Fig. 3. **The lipid droplet fraction of Hep39 cells contains less ADRP, but more TIP47, than Hepswx cells.** Lipid droplet fractions (1.5 μg of protein per lane) from Hepswx and Hep39 cells were analyzed by immunoblotting with the indicated antibodies.

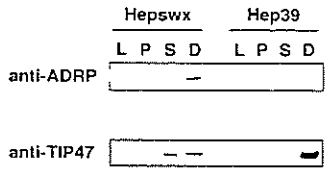

Fig. 4. **Subcellular localization of ADRP and TIP47 in Hepswx and Hep39 cells.** Hepswx and Hep39 cells were fractionated into post-nuclear supernatant (lane L), 100,000 × *g* precipitate (lane P), 100,000 × *g* supernatant (lane S), and lipid droplet (lane D) fractions as described in "MATERIALS AND METHODS." Ten micrograms of protein was processed for gel electrophoresis, and then analyzed by immuonoblotting with anti-ADRP and anti-TIP47 antibodies.

(Fig. 4). The mRNA expression level of ADRP in Hep39 cells was less than half that in Hepswx cells (data not shown), consistent with the immunoblot data shown in Fig. 4. These results suggest that the lower ADRP content in the lipid droplet fraction of Hep39 cells is due to a low expression level of ADRP. In contrast, Hep39 cells had much more TIP47 in the lipid droplet fraction (Figs. 3 and 4, lanes D), but the cellular TIP47 content of Hep39 cells was not more than that in Hepswx cells (Fig. 4, lanes L). Besides the lipid droplet fraction, the cytosolic fraction of Hepswx cells was found to contain TIP47 at a substantial level, while the cytosolic fraction of Hep39 cells did not (Fig. 4, lanes S). These results indicate that the intracellular distribution of TIP47 shifts drastically from the cytosol to lipid droplets in HCV core–expressing Hep39 cells.

Another obvious difference between Hepswx and Hep39 cells in Fig. 2 is the presence of a specific ~85 kDa band (Fig. 2, band 16) in Hep39 cells, which was identified as DEAD box protein 1 (DDX1), a DEAD box protein family member, by 1-D-SDS-PAGE/MALDI-TOF MS analysis (Table 1). DNLC-MS/MS analysis also supported the existence of DDX1 in the lipid droplet fraction of Hep39 cells (Table 2). In addition, DEAD box protein 3 (DDX3), another DEAD box protein family member, was also detected in the lipid droplet fraction of Hep39 cells by means of the two different strategies used for proteomic analysis (Tables 1 and 2), suggesting that DDX3 is a major lipid droplet protein in Hep39 cells. To verify the association of DDX 1 and DDX3 with lipid droplets in Hep39 cells, immunoblot analysis was carried out. Figure 5 shows that DDX 1 and DDX 3 exist in the lipid droplet fraction of HCV core-expressing Hep39 cells, but not Hepswx cells. These results imply the

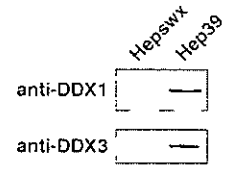

Fig. 5. **Hep39 cells, but not Hepswx cells, have DDX1 and DDX3 in the lipid droplet fraction.** Lipid droplet fractions (0.5 μg of protein per lane) in Hepswx and Hep39 cells were analyzed by immunoblotting with anti-DDX1 and anti-DDX3 antibodies.

special pathological functions of DDX1 and DDX3 in lipid droplets in HCV core–expressing cells.

DISCUSSION

To analyze lipid droplet proteins, we performed proteomic analysis by means of 1-D-SDS-PAGE/MALDI-TOF MS and automated DNLC-MS/MS, and identified 25 and 36 proteins, respectively (Tables 1 and 2). Many more lipid droplet proteins were identified by DNLC-MS/MS, and 22 major proteins separated by 1-D-SDS-PAGE (Fig. 2, bands, 2, 3, 4, 5, 7, 9, 10, 12, 13, 16, 17, 18, 21, 22, 24, 26, 27, 29, and 30) and detected on MALDI-TOF MS analysis were also detected on DNLC-MS/MS analysis. These results indicate that DNLC-MS/MS is a very sensitive and reliable system as well as a high-throughput method. Particularly, DNLC-MS/MS would be a powerful system for exhaustive proteomic analysis of protein mixtures/complexes (up to ~100 proteins) such as lipid droplets.

In our targeted proteomic study, we identified a total of 48 lipid droplet proteins: 30 proteins in control Hepswx cells, 38 proteins in HCV core–expressing Hep39 cells, and 20 proteins in both cell lines. The resident lipid droplet proteins were classified into four groups (Tables 1 and 2), consistent with the recently reported data obtained on proteomic analysis of lipid droplet proteins in other cell lines (*58–60*). In addition, multiple proteins, such as the sterol carrier protein 2–related form, fatty acid binding protein 5, and apoptosis-inducing factor homologous mitochondrion-associated inducer of death, were newly identified as lipid droplet proteins in this study. These accumulated data obtained on proteomic analysis will be useful for understanding the biogenesis and functions of lipid droplets about which little is yet known.

A prominent effect of the expression of HCV core protein on the composition of lipid droplet proteins was observed among the PAT family proteins, i.e. ADRP and TIP47. HCV core–expressing Hep39 cells contained much less ADRP in the lipid droplet fraction (Fig. 3), probably because of the lower cellular expression level and the lack of induction of expression upon lipid loading (data not shown). In contrast, a substantial amount of TIP47 was associated with the lipid droplet fraction of Hep39 cells (Fig. 3). Perilipin, a structural protein of lipid droplets in adipocytes, ADRP, and TIP47, termed PAT family proteins (*61*), share extensive amino acid sequence similarity (*61–63*), suggesting a common biological function in lipid droplet formation. For example, the transition in surface protein composition of lipid droplets from ADRP to perilipin occurs during adipocyte differentiation (*64*). Thus, TIP47 might replace ADRP

on the lipid droplets in Hep39 cells. Cellular TIP47 was not up-regulated in Hep39 cells, resulting in a reduction of TIP47 in the cytosolic fraction (Fig. 4). Since TIP47, originally identified as having the ability to interact with the mannose 6-phosphate/IGF-II receptor (*63*), appears to be essential for the endocytic recycling system (*65–67*), the altered distribution of cellular TIP47 in Hep39 cells could affect intracellular membrane trafficking pathways. Consistent with this assumption, our preliminary results showed that the rate of protein secretion from cells was apparently slower for Hep39 cells than Hepswx cells (unpublished data). Patients chronically infected with HCV (*68*) and HCV core–transgenic mice (*69*) exhibit decreased levels of plasma very low density lipoproteins secreted from the liver, also suggesting interference with intracellular membrane trafficking (secretion pathways) by HCV core proteins. We currently speculate that the reduction in cellular ADRP expression mediated by HCV core protein causes the accumulation of TIP47 in lipid droplets as a substitute, and that the resulting depletion of TIP47 in the cytosol could cause the impairment of intracellular membrane trafficking, followed by the cellular accumulation of membrane lipids and consequent lipid droplet formation. Although further studies remain to be done to confirm these possibilities, we suggest that HCV core protein influences not only the biogenesis of lipid droplets but also intracellular membrane trafficking.

Another interesting finding in this study is that Hep39 cells, unlike Hepswx cells, contain DEAD box proteins, DDX1 and DDX3, as major lipid droplet proteins (Figs. 2 and 5). On the basis of the results of studies involving yeast two-hybrid assays, DDX3 has been shown to be able to interact with HCV core protein, and studies involving immunofluorescent microscopy have revealed that DDX3 is distributed in cytosolic spots such as lipid droplets (*27*, *70*, *71*). These results, together with our present findings, suggest that DDX3 is associated with lipid droplets via HCV core proteins located on lipid droplets. In addition to DDX1 and DDX3, which possess ATPase/RNA helicase activities (*27*, *72*, *73*), several other proteins involved in RNA metabolism/binding, including HC56/gemin 4 and IGF-II mRNA–binding protein 3, were also detected in the lipid droplet fraction of HCV core-expressing Hep39 cells (Tables 1 and 2). Recently Dvorak *et al.* reported that RNA itself can be associated with lipid droplets in human mast cells (*74*). Taken together, these data strongly suggest that lipid droplets containing HCV core proteins may participate in the RNA metabolism of the host and/or HCV in HCV-infected cells. Furthermore, the findings that DDX1 is overexpressed in cell lines derived from tumors such as retinoblastomas and neuroblastomas (*75*), and that cellular expression of DDX3 induces anchorage-independent cell growth (*76*) suggest the involvement of DDX1 and DDX3 in carcinogenesis.

Some groups recently reported profiles of mRNAs up- or down-regulated by expression of the HCV core protein (*77–79*), but these mRNAs included no molecules identified as lipid droplet proteins in this study. Since lipid droplets are a minor organelle in cells, it might be difficult to detect changes in the mRNA expression levels of lipid droplet proteins. The merits of targeted proteomic study are that it is possible to focus on minor cellular fractions, and also to detect changes in the intracellular distributions of proteins. Actually, the mRNA expression levels of TIP47, DDX1, and DDX3 did not change in Hep39 cells (data not shown).

We identified many other lipid droplet proteins found in either Hepswx or Hep39 cells, but their biological functions remain mostly unknown (Tables 1 and 2). Elucidation of the biological functions of these proteins will lead to an advanced understanding of the pathogeneses of HCV-derived liver diseases.

This work was supported by Grants-in-Aid from the Ministry of Health, Labor and Welfare; the program for the Promotion of Fundamental Studies in Health Sciences of the Organization for Drug ADR Relief, R&D Promotion, and Product Review of Japan; the TAKEDA SCIENCE FOUNDATION; and the Integrated Proteomics System Project for Pioneer Research on Genome the Frontier from the Ministry of Education, Culture, Sports, Science & Technology of Japan.

REFERENCES

1. Choo, Q.L., Kuo, G., Weiner, A.J., Overby, L.R., Bradley, D.W., and Houghton, M. (1989) Isolation of a cDNA clone derived from a blood-borne non-A, non-B viral hepatitis genome. *Science* **244**, 359–362
2. Kuo, G., Choo, Q.L., Alter, H.J., Gitnick, G.L., Redeker, A.G., Purcell, R.H., Miyamura, T., Dienstag, J.L., Alter, M.J., Stevens, C.E., Tegtmeier, G.E., Bonino, F., Colombo, M., Lee, W.-S., Kuo, C., Berger, K., Shuster, J.R., Overby, L.R., Bradley, D.W., and Houghton, M. (1989) An assay for circulating antibodies to a major etiologic virus of human non-A, non-B hepatitis. *Science* **244**, 362–364
3. Saito, I., Miyamura, T., Ohbayashi, A., Harada, H., Katayama, T., Kikuchi, S., Watanabe, Y., Koi, S., Onji, M., Ohta, Y., Choo, Q.-L., Houghton, M., and Kuo, G. (1990) Hepatitis C virus infection is associated with the development of hepatocellular carcinoma. *Proc. Natl. Acad. Sci. USA* **87**, 6547–6549
4. Kiyosawa, K., Sodeyama, T., Tanaka, E., Gibo, Y., Yoshizawa, K., Nakano, Y., Furuta, S., Akahane, Y., Nishioka, K., Purcell, R.H., and Alter, H.J. (1990) Interrelationship of blood transfusion, non-A, non-B hepatitis and hepatocellular carcinoma: analysis by detection of antibody to hepatitis C virus. *Hepatology* **12**, 671–675
5. Bartenschlager, R. and Lohmann, V. (2000) Replication of hepatitis C virus. *J. Gen. Virol.* **81**, 1631–1648
6. Grakoui, A., Wychowski, C., Lin, C., Feinstone, S.M., and Rice, C.M. (1993) Expression and identification of hepatitis C virus polyprotein cleavage products. *J. Virol.* **67**, 1385–1395
7. McLauchlan, J., Lemberg, M.K., Hope, G., and Martoglio, B. (2002) Intramembrane proteolysis promotes trafficking of hepatitis C virus core protein to lipid droplets. *EMBO J.* **21**, 3980–3988
8. Okamoto, K., Moriishi, K., Miyamura, T., and Matsuura, Y (2004) Intramembrane proteolysis and endoplasmic reticulum retention of hepatitis C virus core protein. *J. Virol.* **78**, 6370–6380
9. Santolini, E., Migliaccio, G., and La Monica, N. (1994) Biosynthesis and biochemical properties of the hepatitis C virus core protein. *J. Virol.* **68**, 3631–3641
10. Barba, G., Harper. F., Harada, T., Kohara, M. Goulinet. S., Matsuura, Y., Eder, G., Schaff, Z., Chapman. M.J., Miyamura, T., and Brechot, C. (1997) Hepatitis C virus core protein shows a cytoplasmic localization and associates to cellular lipid storage droplets. *Proc. Natl. Acad. Sci. USA* **94**, 1200–1205
11. Ray, R.B., Lagging, L.M., Meyer, K., and Ray, R. (1996) Hepatitis C virus core protein cooperates with ras and transforms

primary rat embryo fibroblasts to tumorigenic phenotype. *J. Virol.* **70**, 4438–4443
12. Yoshida, T., Hanada, T., Tokuhisa, T., Kosai, K., Sata, M., Kohara, M., and Yoshimura, A. (2002) Activation of STAT3 by the hepatitis C virus core protein leads to cellular transformation. *J. Exp. Med.* **196**, 641–653
13. Moriya, K., Yotsuyanagi, H., Shintani, Y., Fujie, H., Ishibashi, K., Matsuura, Y., Miyamura, T., and Koike, K. (1997) Hepatitis C virus core protein induces hepatic steatosis in transgenic mice. *J. Gen. Virol.* **78**, 1527–1531
14. Moriya, K., Fujie, H., Shintani, Y., Yotsuyanagi, H., Tsutsumi, T., Ishibashi, K., Matsuura, Y., Kimura, S., Miyamura, T., and Koike, K. (1998) The core protein of hepatitis C virus induces hepatocellular carcinoma in transgenic mice. *Nat. Med.* **4**, 1065–1067
15. Kim, D.W., Suzuki, R., Harada, T., Saito, I., and Miyamura, T. (1994) Trans-suppression of gene expression by hepatitis C viral core protein. *Jpn. J. Med. Sci. Biol.* **47**, 211–220
16. Ray, R.B., Steele, R., Meyer, K., and Ray, R. (1997) Transcriptional repression of p53 promoter by hepatitis C virus core protein. *J. Biol. Chem.* **272**, 10983–10986
17. Shrivastava, A., Manna, S.K., Ray, R., and Aggarwal, B.B. (1998) Ectopic expression of hepatitis C virus core protein differentially regulates nuclear transcription factors. *J. Virol.* **72**, 9722–9728
18. Chen, C.M., You, L.R., Hwang, L.H., and Lee, Y.H. (1997) Direct interaction of hepatitis C virus core protein with the cellular lymphotoxin-beta receptor modulates the signal pathway of the lymphotoxin-beta receptor. *J. Virol.* **71**, 9417–9426
19. Zhu, N., Khoshnan, A., Schneider, R., Matsumoto, M., Dennert, G., Ware, C., and Lai, M.M. (1998) Hepatitis C virus core protein binds to the cytoplasmic domain of tumor necrosis factor (TNF) receptor 1 and enhances TNF-induced apoptosis. *J. Virol.* **72**, 3691–3697
20. Tsuchihara, K., Hijikata, M., Fukuda, K., Kuroki, T., Yamamoto, N., and Shimotohno, K. (1999) Hepatitis C virus core protein regulates cell growth and signal transduction pathway transmitting growth stimuli. *Virology* **258**, 100–107
21. You, L.R., Chen, C.M., and Lee, Y.H. (1999) Hepatitis C virus core protein enhances NF-kappaB signal pathway triggering by lymphotoxin-beta receptor ligand and tumor necrosis factor alpha. *J. Virol.* **73**, 1672–1681
22. Aoki, H., Hayashi, J., Moriyama, M., Arakawa, Y., and Hino, O. (2000) Hepatitis C virus core protein interacts with 14-3-3 protein and activates the kinase Raf-1. *J. Virol.* **74**, 1736–1741
23. Yoshida, H., Kato, N., Shiratori, Y., Otsuka, M., Maeda, S., Kato, J., and Omata, M. (2001) Hepatitis C virus core protein activates nuclear factor kappa B-dependent signaling through tumor necrosis factor receptor-associated factor. *J. Biol. Chem.* **276**, 16399–16405
24. Matsumoto, M., Hsieh, T.Y., Zhu, N., VanArsdale, T., Hwang, S.B., Jeng, K.S., Gorbalenya, A.E., Lo, S.Y., Ou, J.H., Ware, C.F., and Lai, M.M. (1997) Hepatitis C virus core protein interacts with the cytoplasmic tail of lymphotoxin-beta receptor. *J. Virol.* **71**, 1301–1309
25. Hsieh, T.Y., Matsumoto, M., Chou, H.C., Schneider, R., Hwang, S.B., Lee, A.S., and Lai, M.M. (1998) Hepatitis C virus core protein interacts with heterogeneous nuclear ribonucleoprotein K. *J. Biol. Chem.* **273**, 17651–17659
26. Sabile, A., Perlemuter, G., Bono, F., Kohara, K., Demaugre, F., Kohara, M., Matsuura, Y., Miyamura, T., Brechot, C., and Barba, G. (1999) Hepatitis C virus core protein binds to apolipoprotein AII and its secretion is modulated by fibrates. *Hepatology* **30**, 1064–1076
27. You, L.R., Chen, C.M., Yeh, T.S., Tsai, T.Y., Mai, R.T., Lin, C.H., and Lee, Y.H. (1999) Hepatitis C virus core protein interacts with cellular putative RNA helicase. *J. Virol.* **73**, 2841–2853
28. Jin, D.Y., Wang, H.L., Zhou, Y., Chun, A.C., Kibler, K.V., Hou, Y.D., Kung, H., and Jeang, K.T (2000) Hepatitis C virus core protein-induced loss of LZIP function correlates with cellular transformation. *EMBO J.* **19**, 729–740
29. Wang, F., Yoshida, I., Takamatsu, M., Ishido, S., Fujita, T., Oka, K., and Hotta, H. (2000) Complex formation between hepatitis C virus core protein and p21Waf1/Cip1/Sdi1. *Biochem. Biophys. Res. Commun.* **273**, 479–484
30. Otsuka, M., Kato, N., Lan, K., Yoshida, H., Kato, J., Goto, T., Shiratori, Y., and Omata, M. (2000) Hepatitis C virus core protein enhances p53 function through augmentation of DNA binding affinity and transcriptional ability. *J. Biol. Chem.* **275**, 34122–34130
31. Tsutsumi, T., Suzuki, T., Shimoike, T., Suzuki, R., Moriya, K., Shintani, Y., Fujie, H., Matsuura, Y., Koike, K., and Miyamura, T. (2002) Interaction of hepatitis C virus core protein with retinoid X receptor alpha modulates its transcriptional activity. *Hepatology* **35**, 937–946
32. Hosui, A., Ohkawa, K., Ishida, H., Sato, A., Nakanishi, F., Ueda, K., Takehara, T., Kasahara, A., Sasaki, Y., Hori, M., and Hayashi, N. (2003) Hepatitis C virus core protein differently regulates the JAK-STAT signaling pathway under interleukin-6 and interferon-gamma stimuli. *J. Biol. Chem.* **278**, 28562–28571
33. Ohkawa, K., Ishida, H., Nakanishi, F., Hosui, A., Ueda, K., Takehara, T., Hori, M., and Hayashi, N. (2004) Hepatitis C virus core functions as a suppressor of cyclin-dependent kinase-activating kinase and impairs cell cycle progression. *J. Biol. Chem.* **279**, 11719–11726
34. Alisi, A., Giambartolomei, S., Cupelli, F., Merlo, P., Fontemaggi, G., Spaziani, A., and Balsano, C. (2003) Physical and functional interaction between HCV core protein and the different p73 isoforms. *Oncogene* **22**, 2573–2580
35. Okabe, H., Satoh, S., Kato, T., Kitahara, O., Yanagawa, R., Yamaoka, Y., Tsunoda, T., Furukawa, Y., and Nakamura, Y. (2001) Genome-wide analysis of gene expression in human hepatocellular carcinomas using cDNA microarray: identification of genes involved in viral carcinogenesis and tumor progression. *Cancer Res.* **61**, 2129–2137
36. Shirota, Y., Kaneko, S., Honda, M., Kawai, H.F., and Kobayashi, K. (2001) Identification of differentially expressed genes in hepatocellular carcinoma with cDNA microarrays. *Hepatology* **33**, 832–840
37. Iizuka, N., Oka, M., Yamada-Okabe, H., Mori, N., Tamesa, T., Okada, T., Takemoto, N., Tangoku, A., Hamada, K., Nakayama, H., Miyamoto, T., Uchimura, S., and Hamamoto, Y. (2002) Comparison of gene expression profiles between hepatitis B virus- and hepatitis C virus-infected hepatocellular carcinoma by oligonucleotide microarray data on the basis of a supervised learning method. *Cancer Res.* **62**, 3939–3944
38. Iizuka, N., Oka, M., Yamada-Okabe, H., Mori, N., Tamesa, T., Okada, T., Takemoto, N., Hashimoto, K., Tangoku, A., Hamada, K., Nakayama, H., Miyamoto, T., Uchimura, S., and Hamamoto, Y. (2003) Differential gene expression in distinct virologic types of hepatocellular carcinoma: association with liver cirrhosis. *Oncogene* **22**, 3007–3014
39. Smith, M.W., Yue, Z.N., Geiss, G.K., Sadovnikova, N.Y., Carter, V.S., Boix, L., Lazaro, C.A., Rosenberg, G.B., Bumgarner, R.E., Fausto, N., Bruix, J., and Katze, M.G. (2003) Identification of novel tumor markers in hepatitis C virus-associated hepatocellular carcinoma. *Cancer Res.* **63**, 859–864
40. Smith, M.W., Yue, Z.N., Korth, M.J., Do, H.A., Boix, L., Fausto, N. Bruix, J., Carithers, R.L., Jr., and Katze, M.G. (2003) Hepatitis C virus and liver disease: global transcriptional profiling and identification of potential markers. *Hepatology* **38**, 1458–1467
41. Takashima, M., Kuramitsu, Y., Yokoyama, Y Iizuka, N., Toda, T Sakaida, I., Okita, K., Oka, M., and Nakamura, K. (2003) Proteomic profiling of heat shock protein 70 family members as biomarkers for hepatitis C virus-related hepatocellular carcinoma. *Proteomics* **3**, 2487–2493

42. Yokoyama, Y., Kuramitsu, Y., Takashima, M., Iizuka, N., Toda, T., Terai, S., Sakaida, I., Oka, M., Nakamura, K., and Okita, K. (2004) Proteomic profiling of proteins decreased in hepatocellular carcinoma from patients infected with hepatitis C virus. *Proteomics* **4**, 2111–2116
43. Moradpour, D., Englert, C., Wakita, T., and Wands, J.R. (1996) Characterization of cell lines allowing tightly regulated expression of hepatitis C virus core protein. *Virology* **222**, 51–63
44. Hope, R.G. and McLauchlan, J. (2000) Sequence motifs required for lipid droplet association and protein stability are unique to the hepatitis C virus core protein. *J. Gen. Virol.* **81**, 1913–1925
45. Hope, R.G., Murphy, D.J., and McLauchlan, J. (2002) The domains required to direct core proteins of hepatitis C virus and GB virus-B to lipid droplets share common features with plant oleosin proteins. *J. Biol. Chem.* **277**, 4261–4270
46. Shi, S.T., Polyak, S.J., Tu, H., Taylor, D.R., Gretch, D.R., and Lai, M.M. (2002) Hepatitis C virus NS5A colocalizes with the core protein on lipid droplets and interacts with apolipoproteins. *Virology* **292**, 198–210
47. Harada, T., Kim, D.W., Sagawa, K., Suzuki, T., Takahashi, K., Saito, I., Matsuura, Y., and Miyamura, T. (1995) Characterization of an established human hepatoma cell line constitutively expressing non-structural proteins of hepatitis C virus by transfection of viral cDNA. *J. Gen. Virol.* **76**, 1215–1221
48. Balch, W.E. and Rothman, J.E. (1985) Characterization of protein transport between successive compartments of the Golgi apparatus: asymmetric properties of donor and acceptor activities in a cell-free system. *Arch. Biochem. Biophys.* **240**, 413–425
49. Yanagida, M., Miura, Y., Yagasaki, K., Taoka, M., Isobe, T., and Takahashi, N. (2000) Matrix assisted laser desorption/ionization-time of flight-mass spectrometry analysis of proteins detected by anti-phosphotyrosine antibody on two-dimensional-gels of fibrolast cell lysates after tumor necrosis factor-alpha stimulation. *Electrophoresis* **21**, 1890–1898
50. Yanagida, M., Shimamoto, A., Nishikawa, K., Furuichi, Y., Isobe, T., and Takahashi, N. (2001) Isolation and proteomic characterization of the major proteins of the nucleolin-binding ribonucleoprotein complexes. *Proteomics* **1**, 1390–1404
51. Bligh, E.G. and Dyer, W.J. (1959) A rapid method of total lipid extraction and purification. *Can. J. Med. Sci.* **37**, 911–917
52. Natsume, T., Yamauchi, Y., Nakayama, H., Shinkawa, T., Yanagida, M., Takahashi, N., and Isobe, T. (2002) A direct nanoflow liquid chromatography-tandem mass spectrometry system for interaction proteomics. *Anal. Chem.* **74**, 4725–4733
53. Yanagida, M., Hayano, T., Yamauchi, Y., Shinkawa, T., Natsume, T., Isobe, T., and Takahashi, N. (2004) Human fibrillarin forms a sub-complex with splicing factor 2-associated p32, protein arginine methyltransferases, and tubulins alpha 3 and beta 1 that is independent of its association with preribosomal ribonucleoprotein complexes. *J. Biol. Chem.* **279**, 1607–1614
54. Heid, H.W., Moll, R., Schwetlick, I., Rackwitz, H.R., and Keenan, T.W. (1998) Adipophilin is a specific marker of lipid accumulation in diverse cell types and diseases. *Cell Tissue Res.* **294**, 309–321
55. Londos, C., Brasaemle, D.L., Schultz, C.J., Segrest, J.P., and Kimmel, A.R. (1999) Perilipins, ADRP, and other proteins that associate with intracellular neutral lipid droplets in animal cells. *Semin. Cell Dev. Biol.* **10**, 51–58
56. Wolins, N.E., Rubin, B. and Brasaemle, D.L. (2001) TIP47 associates with lipid droplets. *J. Biol. Chem.* **276**, 5101–5108
57. Miura, S., Gan, J.W., Brzostowski, J., Parisi, M.J. Schultz, C.J., Londos, C. Oliver, B., and Kimmel, A.R. (2002) Functional conservation for lipid storage droplet association among Perilipin, ADRP, and TIP47 (PAT)-related proteins in mammals, Drosophila, and Dictyostelium. *J. Biol. Chem.* **277**, 32253–32257
58. Liu, P., Ying, Y., Zhao, Y., Mundy, D.I., Zhu, M., and Anderson, R.G. (2004) Chinese hamster ovary K2 cell lipid droplets appear to be metabolic organelles involved in membrane traffic. *J. Biol. Chem.* **279**, 3787–3792
59. Fujimoto, Y., Itabe, H., Sakai, J., Makita, M., Noda, J., Mori, M., Higashi, Y., Kojima, S., and Takano, T. (2004) Identification of major proteins in the lipid droplet-enriched fraction isolated from the human hepatocyte cell line HuH7. *Biochim. Biophys. Acta* **1644**, 47–59
60. Brasaemle, D.L., Dolios, G., Shapiro, L., and Wang, R. (2004) Proteomic analysis of proteins associated with lipid droplets of basal and lipolytically stimulated 3T3-L1 adipocytes. *J. Biol. Chem.* **279**, 46835–46842
61. Lu, X., Gruia-Gray, J., Copeland, N.G., Gilbert, D.J., Jenkins, N.A., Londos, C., and Kimmel, A.R. (2001) The murine perilipin gene: the lipid droplet-associated perilipins derive from tissue-specific, mRNA splice variants and define a gene family of ancient origin. *Mamm. Genome* **12**, 741–749
62. Greenberg, A.S., Egan, J.J., Wek, S.A., Moos, M.C., Jr., Londos, C., and Kimmel, A.R. (1993) Isolation of cDNAs for perilipins A and B: sequence and expression of lipid droplet-associated proteins of adipocytes. *Proc. Natl. Acad. Sci. USA* **90**, 12035–12039
63. Diaz, E. and Pfeffer, S.R. (1998) TIP47: a cargo selection device for mannose 6-phosphate receptor trafficking. *Cell* **93**, 433–443
64. Brasaemle, D.L., Barber, T., Wolins, N.E., Serrero, G., Blanchette-Mackie, E.J., and Londos, C. (1997) Adipose differentiation-related protein is an ubiquitously expressed lipid storage droplet-associated protein. *J. Lipid Res.* **38**, 2249–2263
65. Carroll, K.S., Hanna, J., Simon, I., Krise, J., Barbero, P., and Pfeffer, S.R. (2001) Role of Rab9 GTPase in facilitating receptor recruitment by TIP47. *Science* **292**, 1373–1376
66. Pfeffer, S.R. (2001) Rab GTPases: specifying and deciphering organelle identity and function. *Trends Cell Biol.* **11**, 487–491
67 Blot, G., Janvier, K., Le Panse, S., Benarous, R., and Berlioz-Torrent, C. (2003) Targeting of the human immunodeficiency virus type 1 envelope to the trans-Golgi network through binding to TIP47 is required for env incorporation into virions and infectivity. *J. Virol.* **77**, 6931–6945
68. Serfaty, L., Andreani, T., Giral, P., Carbonell, N., Chazouilleres, O., and Poupon, R. (2001) Hepatitis C virus induced hypobetalipoproteinemia: a possible mechanism for steatosis in chronic hepatitis C. *J. Hepatol.* **34**, 428–434
69. Perlemuter, G., Sabile, A., Letteron, P., Vona, G., Topilco, A., Chretien, Y., Koike, K., Pessayre, D., Chapman, J., Barba, G., and Brechot, C. (2002) Hepatitis C virus core protein inhibits microsomal triglyceride transfer protein activity and very low density lipoprotein secretion: a model of viral-related steatosis. *FASEB J.* **16**, 185–194
70. Owsianka, A.M. and Patel, A.H. (1999) Hepatitis C virus core protein interacts with a human DEAD box protein DDX3. *Virology* **257**, 330–340
71. Mamiya, N. and Worman, H.J. (1999) Hepatitis C virus core protein binds to a DEAD box RNA helicase. *J. Biol. Chem.* **274**, 15751–15756
72. Gururajan, R. and Weeks, D.L. (1997) An3 protein encoded by a localized maternal mRNA in Xenopus laevis is an ATPase with substrate-specific RNA helicase activity. *Biochim. Biophys. Acta* **1350**, 169–182
73. Chen, H.C., Lin, W.C., Tsay, Y.G., Lee, S.C., and Chang, C.J. (2002) An RNA helicase. DDX1, interacting with poly(A) RNA and heterogeneous nuclear ribonucleoprotein K. *J. Biol. Chem.* **277**, 40403–40409
74. Dvorak, A.M., Morgan, E.S., and Weller, P.F (2003) RNA is closely associated with human mast cell lipid bodies. *Histol. Histopathol.* **18**, 943–968
75. Godbout, R., Packer, M., and Bie, W. (1998) Overexpression of a DEAD box protein (DDX1) in neuroblastoma and retinoblastoma cell lines. *J. Biol. Chem.* **273**, 21161–21168

76. Huang, J.S., Chao, C.C., Su, T.L., Yeh, S.H., Chen, D.S., Chen, C.T., Chen, P.J., and Jou, Y.S. (2004) Diverse cellular transformation capability of overexpressed genes in human hepatocellular carcinoma. *Biochem. Biophys. Res. Commun.* **315**, 950–958
77. Liu, M., Liu, Y., Cheng, J., Zhang, S.L., Wang, L., Shao, Q., Zhang, J., and Yang, Q. (2004) Transactivating effect of hepatitis C virus core protein: a suppression subtractive hybridization study. *World J. Gastroenterol.* **10**, 1746–1749
78. Ohkawa, K., Ishida, H., Nakanishi, F., Hosui, A., Sato, A., Ueda, K., Takehara, T., Kasahara, A., Sasaki, Y., Hori, M., and Hayashi, N. (2003) Changes in gene expression profile by HCV core protein in cultured liver cells: analysis by DNA array assay. *Hepatol. Res.* **25**, 396–408
79. Sacco, R., Tsutsumi, T., Suzuki, R., Otsuka, M., Aizaki, H., Sakamoto, S., Matsuda, M., Seki, N., Matsuura, Y., Miyamura, T., and Suzuki, T. (2003) Antiapoptotic regulation by hepatitis C virus core protein through up-regulation of inhibitor of caspase-activated DNase. *Virology* **317**, 24–35

Enhancement of *de Novo* Fatty Acid Biosynthesis in Hepatic Cell Line Huh7 Expressing Hepatitis C Virus Core Protein

Masayoshi FUKASAWA,*[,a] Yasuhito TANAKA,[a] Shigeko SATO,[a] Yujin ONO,[a] Yuko NITAHARA-KASAHARA,[a] Tetsuro SUZUKI,[b] Tatsuo MIYAMURA,[b] Kentaro HANADA,[a] and Masahiro NISHIJIMA[a,c]

[a] *Department of Biochemistry and Cell Biology, National Institute of Infectious Diseases; and* [b] *Department of Virology II, National Institute of Infectious Diseases; Tokyo 162–8640, Japan: and* [c] *Department of Clinical Pharmacy, Faculty of Pharmaceutical Sciences, Doshisha Women's College of Liberal Arts; Kyoto 610–0395, Japan.*
Received June 12, 2006; accepted July 7, 2006; published online July 10, 2006

Hepatitis C virus (HCV) core protein plays important roles in the pathogeneses of liver steatosis as well as hepatocellular carcinomas due to HCV infection. In this study, we examined *de novo* fatty acid biosynthesis in hepatic cell line Huh7 cells expressing HCV core protein. The rate of metabolic labeling of cellular fatty acids with [^{3}H]acetate in core-expressing (Uc39-6) cells was *ca.* 1.5-fold higher than that in non-expressing (Uc321) cells. The enzyme activities responsible for fatty acid biosynthesis were assayed *in vitro*. Cytosolic acetyl-CoA carboxylase activity in Uc39-6 cells was *ca.* 1.6-fold higher than that in Uc321 cells. On the other hand, cytosolic fatty acid synthase activity in Uc39-6 cells was only slightly higher than that in Uc321 cells. Immunoblot analysis of acetyl-CoA carboxylase 1 (ACC1), which is a rate-limiting enzyme for fatty acid biosynthesis, revealed a higher expression level of the protein in Uc39-6 cells than in Uc321 cells. The ACC1 mRNA content in Uc39-6 cells was 1.4-fold higher than that in Uc321 cells. These results strongly suggest that enhancement of fatty acid biosynthesis in core-expressing cells is caused by increased expression of fatty acid biosynthetic enzymes, especially ACC1. Up-regulation of *de novo* fatty acid biosynthesis by HCV core protein may affect cellular lipid metabolism, resulting in neutral lipid accumulation in HCV-infected cells.

Key words fatty acid biosynthesis; hepatitis C virus; acetyl-CoA carboxylase; fatty acid synthase

Hepatitis C virus (HCV) is a major causative agent of chronic hepatitis.[1,2] Persistent HCV infection, which develops in at least 70 to 80% of infected patients, is strongly correlated with the development of severe liver diseases such as cirrhosis and hepatocellular carcinomas (HCC).[3,4] In addition, liver steatosis, which involves the accumulation of intracellular neutral lipids as lipid droplets, is a hallmark of chronic HCV infection,[5] and is suggested to play a central role in the progression of the following liver cirrhosis and HCC in chronic hepatitis C patients.[6] Since more than 170 million people in the world are currently infected with HCV,[1] understanding the mechanisms by which HCV induces serious liver diseases is one of the most important global public health issues.

HCV, belonging to the *Flaviviridae* family, possesses a linear, positive-stranded RNA genome of *ca.* 9600 nucleotides.[7] The HCV genome has a single open reading frame encoding a precursor polyprotein of *ca.* 3000 amino acids that is processed into at least 10 individual proteins by host and viral proteases.[8] HCV core protein, the product of the N-terminal portion of the polyprotein, forms the nucleocapsid of an HCV virion.[9] Besides its function as a viral structural protein, the core protein causes intracellular lipid accumulation as well as malignant transformation in cultured cells.[10—13] Moreover, transgenic mice expressing HCV core protein developed liver steatosis and the following HCC.[14,15] These results strongly suggest that HCV core protein is involved in the pathogeneses of liver diseases including steatosis due to HCV infection.

The details of the mechanisms by which HCV core protein causes intracellular neutral lipid accumulation are not well understood. Extensive screening for genes/proteins exhibiting differences in cellular expression involving cDNA microarray or proteome analysis has been performed for HCV core-expressing cultured liver cells or transgenic mice.[16—19] Although various genes/proteins were identified, direct information on the genes/proteins related to lipid metabolism altered by HCV core protein expression has not been obtained yet. Since HCV core protein is distributed mainly in lipid droplets of host cells,[10,13,20—23] the biogenesis and/or functions of lipid droplets might be affected by the core protein. As reported, the core protein appears to inhibit microsomal triglyceride transfer protein activity in the livers of HCV core-transgenic mice, thus interfering with the hepatic assembly and secretion of apo-B-carrying very low density lipoproteins.[24] As a result, triglycerides appear to accumulate within hepatocytes, steatosis developing. HCV core protein also interacts with apoA2, a major component of high-density lipoproteins, in cells.[10,25] These results should be important regarding the pathogenesis of HCV core-derived steatosis, but may not explain all the functions of the core protein causing intracellular neutral lipid accumulation. In this study, we investigated *de novo* fatty acid biosynthesis, which can significantly affect intracellular lipid metabolism, especially neutral lipid accumulation,[26,27] in HCV core-expressing liver cells. We found elevated fatty acid biosynthesis, and higher expression and activities of the enzymes responsible for *de novo* fatty acid biosynthesis in HCV core-expressing cells.

MATERIALS AND METHODS

Cell Lines The human hepatic Huh7 cell line constitutively expressing HCV core protein (Uc39-6) was established by transfection with pcEF39neo.[28] Expression level of HCV core protein in Uc39-6 cells was similar to that in core-expressing Hep39 cells (data not shown), which we established previously.[28,29] Another Huh7 cell line transfected with ex-

* To whom correspondence should be addressed. e-mail: fuka@nih.go.jp

pression vector pcEF321swxneo[28] without the HCV core protein insert (Uc321) was used as a mock control. Both cell lines were plated on collagen-coated dishes (Asahi Techno Glass, Japan) and maintained in normal culture medium (DMEM supplemented with 10% fetal bovine serum, 100 units/ml penicillin G, 100 μg/ml streptomycin sulfate, and 1 mg/ml G418 (Sigma, U.S.A.)) under a 5% CO_2 atmosphere at 37°C. Growth rates under the culture condition we used were comparable between Uc321 and Uc39-6 cells.

Metabolic Labeling of Cellular Lipids Subconfluent cell monolayers in 6-cm dishes were incubated in 2 ml of the normal medium containing 1.3 μM [^{3}H]acetate (Moravek Biochemicals, U.S.A.) for various times. After being washed three times with 3 ml of PBS, the cells were lysed in 1 ml of 0.1% SDS at 4°C, and then 100 and 800 μl aliquots of the resultant cell lysate were used for protein determination and lipid extraction, respectively. Cellular lipids were extracted into the organic solvent[30] and dried up. To determine the total metabolic incorporation of [^{3}H]acetate into the fatty acid moieties of lipids, the extracted lipids were treated with 90% ethanol containing 1 N KOH for 1 h at 70°C and then re-extracted with petroleum ether. Fatty acids were then separated on TLC plates with a solvent system of hexane/diethylether/acetate (70/30/1, vol/vol). The radioactivity of fatty acids was determined with a BAS1800 imaging analysis system (Fuji Film, Japan). The values were normalized as to cell protein.

***In Vitro* Acetyl-CoA Carboxylase (ACC) and Fatty Acid Synthase (FAS) Activity Assays** ACC activity assays were performed using [^{14}C] $KHCO_3$ (American Radiolabeled Chemicals, U.S.A.).[31] FAS activity was measured using [^{14}C]acetyl-CoA (Moravek Biochemicals, U.S.A.).[32] Cytosolic fractions, which contain ACC1 and FAS, were prepared as below. After being washed with PBS, cells were harvested and precipitated by centrifugation (300×g, 5 min). The precipitated cells were resuspended in 125 mM potassium phosphate, pH 7.0, and then lysed by sonication. After centrifugation of each lysate at 2500×g for 5 min, the cytosolic fraction (supernatant) was separated from the post-nuclear supernatant by centrifugation at 100000×g for 60 min. The protein concentrations of the preparations were determined with a BCA protein assay kit (Pierce, U.S.A.).

Immunoblot Analysis Equivalent amounts of proteins from Uc321 and Uc39-6 cells were separated in a 4—12% SDS-polyacrylamide gel and then electrophoretically transferred to polyvinylidene difluoride membranes. The membranes were blocked overnight at 4°C in TBS containing 0.1% Tween 20 and 5% skim milk. The blots were probed with a rabbit polyclonal anti-ACC1 antibody (Upstate, U.S.A.) (1 : 1000), a mouse monoclonal anti-FAS antibody (BD Transduction Laboratories, U.S.A.) (1 : 1000), and a mouse monoclonal anti-HCV core protein antibody (Anogen, Canada) (1 : 2000) for 90 min at room temperature. The blots were then incubated with horseradish peroxidase-conjugated goat anti-rabbit IgG (BIO-RAD, U.S.A.), or HRP-conjugated goat anti-mouse IgG (GE Healthcare, U.S.A.) at 1 : 2000 dilution for 60 min. Detection of immunoreactive proteins was performed with an ECL system (GE Healthcare, U.S.A.).

Quantitative Real-Time PCR Analysis Cellular total RNAs were prepared with an RNeasy kit (Qiagen, U.S.A.). The total RNA fraction (1 μg) was processed directly to cDNA using a Transcriptor First Strand cDNA Synthesis Kit (Roche, U.S.A.). Of the total 20 μl cDNA solution, an aliquot of 0.5 μl was used for each real-time PCR assay. The PCR primers used for human ACC1 were: forward, CTGTTGGCTCAGATACACTC, and reverse, GCCACAGTGAAATCTCGTT. The PCR primers for human FAS were: forward, GTGGGAAGGTGTACCAGTG, and reverse, AGGATGCCCTGGAAATGAG. Quantitative real-time PCR was carried out in a LightCycler (Roche, U.S.A.) using LightCycler-FastStart DNA Master SYBR Green I (Roche, U.S.A.). Specific PCR products amplified against individual genes were used as quantitative standards.

RESULTS

To determine the effect of HCV core protein expression on cellular fatty acid biosynthesis, we established Uc39-6 cells, a human hepatic Huh7 cell line transfected with the pcEF321 mammalian expression vector containing the HCV core protein gene, and Uc321 cells, a control Huh7 cell line transfected with the pcEF321 vector without the core protein gene. Consistent with previous studies involving HCV core-expressing hepatic cell lines,[10,33] HCV core protein was preferentially distributed in the endoplasmic reticulum and lipid droplets in Uc39-6 cells, as determined on immunofluorescence microscopy (data not shown). *De novo* fatty acid biosynthesis in HCV core-expressing and non-expressing cells was examined by metabolic labeling with [^{3}H]acetate. Most biosynthesized [^{3}H]fatty acids were rapidly incorporated into complex lipids such as phospholipids, triglycerides, and cholesteryl esters, but free [^{3}H]fatty acids were not detectable (<1/1000 of total [^{3}H]fatty acids formed) in these cells. Incorporation of radioactivity into the fatty acid moieties of complex lipids was *ca.* 1.5-fold higher in HCV core-expressing Uc39-6 cells than that in non-expressing Uc321 cells during the incubation time at 37°C (Fig. 1). Similar results were obtained with other Huh7 cell lines expressing HCV core protein (data not shown), ruling out the possibility that the increase in radiolabeled fatty acids in HCV core-expressing cells are due to the peculiar cell clones. These results indicate that the rate of *de novo* biosynthesis of cellular fatty acids is enhanced in HCV core-expressing cells.

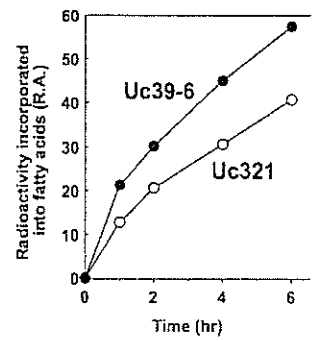

Fig. 1. Fatty Acid Biosynthesis in HCV Core-Expressing Uc39-6 and Control Uc321 Cells

Cells were metabolically labeled with [^{3}H]acetate for the indicated times. The radioactivity incorporated into the fatty acid moieties of lipids was determined as described under Materials and Methods. Open circles, Uc321 cells; closed circles, Uc39-6 cells. R.A., relative radioactivity. Data are representative of four independent experiments.

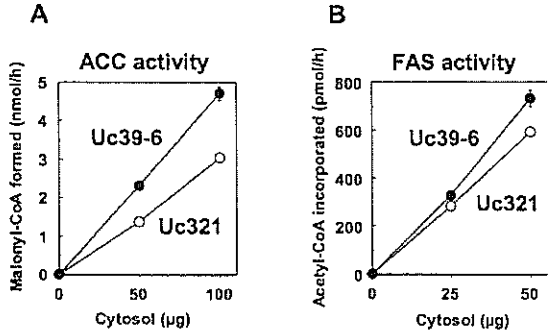

Fig. 2. ACC and FAS Activities in Uc321 and Uc39-6 Cytosolic Fractions

In vitro activity assaying of ACC (A) and FAS (B) was performed as described under Materials and Methods. Open circles, Uc321 cells; closed circles, Uc39-6 cells. Data are expressed as means±S.D. for three determinations.

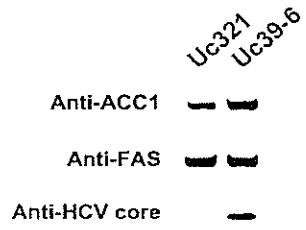

Fig. 3. Immunoblot Analysis of ACC1 and FAS in Uc321 and Uc39-6 Cells

Total cell lysates (30 μg of protein per lane) of Uc321 and Uc39-6 cells were analyzed by immunoblotting with anti-ACC1, anti-FAS, and anti-HCV core antibodies.

Fatty acid biosynthesis is carried out by cytosolic enzymes, *i.e.*, ACC1 and FAS.[34] We assayed these enzyme activities in cytosolic fractions of Uc321 and Uc39-6 cells. HCV core-expressing Uc39-6 cells showed a *ca.*1.6-fold higher level of ACC activity than Uc321 cells (Fig. 2A). The cytosolic FAS activity in Uc39-6 cells was slightly higher than that in Uc321 cells (Fig. 2B). These results demonstrate that the enzymatic activities responsible for fatty acid biosynthesis, especially ACC activity, are elevated in HCV core-expressing Uc39-6 cells, consistent with the results of metabolic labeling experiments involving [^{3}H]acetate.

Cytosolic ACC and FAS activities are attributed to ACC1 and FAS molecules, respectively.[34] We next performed immunoblot analyses of ACC1 and FAS molecules in lysates of Uc321 and Uc39-6 cells. Uc39-6 cells contained a *ca.* 2-fold higher amount of ACC1 protein than Uc321 cells (Fig. 3), whereas the protein level of FAS in UC39-6 cells was comparable to that in Uc321 cells. These results suggest that the elevated protein level of ACC1, a rate-limiting enzyme for fatty acid biosynthesis, may contribute to the higher ACC activity, leading to enhanced fatty acid biosynthesis, in HCV core-expressing Uc39-6 cells. We also determined the mRNA levels of ACC1 and FAS in Uc321 and Uc39-6 cells by quantitative real-time PCR. Consistent with the protein levels of ACC1, the ACC1 mRNA content in Uc39-6 cells was significantly higher than that in Uc321 cells (Fig. 4A). The FAS mRNA content in Uc39-6 cells was also higher than that in Uc321 cells (Fig. 4B). These results suggest that elevated expression of the ACC1 (and FAS) gene(s) causes a higher rate of *de novo* fatty acid biosynthesis in HCV core-expressing cells.

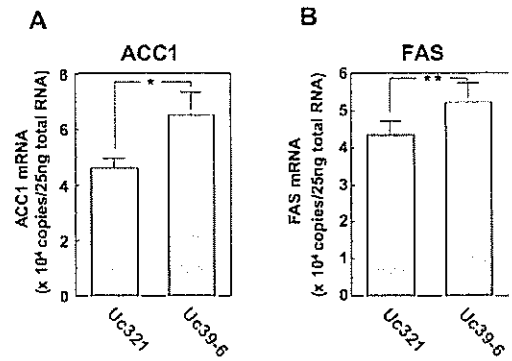

Fig. 4. ACC1 and FAS mRNA Levels in Uc321 and Uc39-6 Cells

Total RNA was isolated from Uc321 and Uc39-6 cells, and the ACC1 (A) and FAS (B) mRNA levels were determined by quantitative real-time PCR. Data are expressed as means±S.D. for three determinations. Statistical significance of differences in mRNA levels between Uc321 and Uc39-6 cells was evaluated using Student's *t* test. $*p<0.01$, $**p<0.025$.

DISCUSSION

In this study we showed that the rate of *de novo* fatty acid biosynthesis was elevated in HCV core-expressing cells (Fig. 1). We also demonstrated that the protein and mRNA expression levels as well as the *in vitro* enzymatic activity of ACC1, which is a rate-limiting key enzyme for fatty acid biosynthesis, were significantly enhanced in HCV core-expressing Uc39-6 cells (Figs. 2—4). These results strongly suggest that the higher expression of ACC1 contributes to the increased fatty acid biosynthesis in HCV core-expressing cells.

Many studies have demonstrated that HCV core protein substantially affects various cellular regulatory processes including gene transcription.[35—37] These biological activities of HCV core protein might be involved in the mechanism by which HCV core protein enhances expression of the ACC1 gene.

HCV core protein is localized mainly in lipid droplets of host cells,[10,13,20—23] and a small portion of ACC1 molecules is also associated with lipid droplets.[38] It is well known that the activity of ACC1 can be regulated posttranslationally through its phosphorylation, and allosteric effectors such as citrate and fatty acids.[39] Thus, we can not exclude the possibility that HCV core protein activates ACC1 directly in lipid droplets, although we have not examined this yet.

We also found that the FAS mRNA expression level was slightly enhanced, but the protein level as well as the *in vitro* enzymatic activity of FAS were not significantly elevated in Uc39-6 cells (Figs. 2—4). FAS appears to make a lesser contribution to the enhancement of fatty acid biosynthesis in Uc39-6 cells under our culture conditions, although further investigations are needed.

We think that our findings may provide a new insight into the metabolic pathways for lipids by which HCV core protein causes steatosis, one of the characteristic indications of chronic hepatitis C infection. Although in the future we have to determine whether or not our *in vitro* findings are applicable to an *in vivo* situation on HCV infection, inhibition of ACC1 and/or FAS activity might be effective for preventing the liver steatosis due to HCV infection.

Acknowledgements This work was supported by

Grants-in-Aid from the Ministry of Health, Labor and Welfare; the program for the Promotion of Fundamental Studies in Health Sciences of the Organization for Drug ADR Relief, R&D Promotion, and Product Review of Japan; the Takeda Science Foundation; and the Viral Hepatitis Research Foundation of Japan.

REFERENCES AND NOTES

1) Choo Q. L., Kuo G., Weiner A. J., Overby L. R., Bradley D. W., Houghton M., *Science*, **244**, 359—362 (1989).
2) Kuo G., Choo Q. L., Alter H. J., Gitnick G. L., Redeker A. G., Purcell R. H., Miyamura T., Dienstag J. L., Alter M. J., Stevens C. E., Tegtmeier G. E., Bonino F., Colombo M., Lee W.-S., Kuo C., Berger K., Shuster J. R., Overby L. R., Bradley D. W., Houghton M., *Science*, **244**, 362—364 (1989).
3) Saito I., Miyamura T., Ohbayashi A., Harada H., Katayama T., Kikuchi S., Watanabe Y., Koi S., Onji M., Ohta Y., Choo Q.-L., Houghton M., Kuo G., *Proc. Natl. Acad. Sci. U.S.A.*, **87**, 6547—6549 (1990).
4) Kiyosawa K., Sodeyama T., Tanaka E., Gibo Y., Yoshizawa K., Nakano Y., Furuta S., Akahane Y., Nishioka K., Purcell R. H., Alter H. J., *Hepatology*, **12**, 671—675 (1990).
5) Goodman Z. D., Ishak K. G., *Semin. Liver Dis.*, **15**, 70—81 (1995).
6) Adinolfi L. E., Durante-Mangoni E., Zampino R., Ruggiero G., *Aliment. Pharmacol. Ther.*, **22** (Suppl. 2), 52—55 (2005).
7) Bartenschlager R., Lohmann V., *J. Gen. Virol.*, **81**, 1631—1648 (2000).
8) Grakoui A., Wychowski C., Lin C., Feinstone S. M., Rice C. M., *J. Virol.*, **67**, 1385—1395 (1993).
9) Santolini E., Migliaccio G., La Monica N., *J. Virol.*, **68**, 3631—3641 (1994).
10) Barba G., Harper F., Harada T., Kohara M., Goulinet S., Matsuura Y., Eder G., Schaff Z., Chapman M. J., Miyamura T., Brechot C., *Proc. Natl. Acad. Sci. U.S.A.*, **94**, 1200—1205 (1997).
11) Ray R. B., Lagging L. M., Meyer K., Ray R., *J. Virol.*, **70**, 4438—4443 (1996).
12) Yoshida T., Hanada T., Tokuhisa T., Kosai K., Sata M., Kohara M., Yoshimura A., *J. Exp. Med.*, **196**, 641—653 (2002).
13) Moradpour D., Englert C., Wakita T., Wands J. R., *Virology*, **222**, 51—63 (1996).
14) Moriya K., Yotsuyanagi H., Shintani Y., Fujie H., Ishibashi K., Matsuura Y., Miyamura T., Koike K., *J. Gen. Virol.*, **78**, 1527—1531 (1997).
15) Moriya K., Fujie H., Shintani Y., Yotsuyanagi H., Tsutsumi T., Ishibashi K., Matsuura Y., Kimura S., Miyamura T., Koike K., *Nat. Med.*, **4**, 1065—1067 (1998).
16) Sacco R., Tsutsumi T., Suzuki R., Otsuka M., Aizaki H., Sakamoto S., Matsuda M., Seki N., Matsuura Y., Miyamura T., Suzuki T., *Virology*, **317**, 24—35 (2003).
17) Li K., Prow T., Lemon S. M., Beard M. R., *Hepatology*, **35**, 1237—1246 (2002).
18) Liu M., Zhang S. L., Cheng J., Liu Y., Wang L., Shao Q., Zhang J., Lin S. M., *World J. Gastroenterol.*, **11**, 3351—3356 (2005).
19) Yamaguchi A., Tazuma S., Nishioka T., Ohishi W., Hyogo H., Nomura S., Chayama K., *Dig. Dis. Sci.*, **50**, 1361—1371 (2005).
20) Hope R. G., McLauchlan J., *J. Gen. Virol.*, **81**, 1913—1925 (2000).
21) Hope R. G., Murphy D. J., McLauchlan J., *J. Biol. Chem.*, **277**, 4261—4270 (2002).
22) Shi S. T., Polyak S. J., Tu, H., Taylor D. R., Gretch D. R., Lai, M. M., *Virology*, **292**, 198—210 (2002).
23) McLauchlan J., Lemberg M. K., Hope G., Martoglio B., *EMBO J.*, **21**, 3980—3988 (2002).
24) Perlemuter G., Sabile A., Letteron P., Vona G., Topilco A., Chretien Y., Koike K., Pessayre D., Chapman J., Barba G., Brechot C., *FASEB J.*, **16**, 185—194 (2002).
25) Sabile A., Perlemuter G., Bono F., Kohara K., Demaugre F., Kohara M., Matsuura Y., Miyamura T., Brechot C., Barba G., *Hepatology*, **30**, 1064—1076 (1999).
26) Girard J., Perdereau D., Foufelle F., Prip-Buus C., Ferre P., *FASEB J.*, **8**, 36—42 (1994).
27) Korczynska J., Stelmanska E., Nogalska A., Szolkiewicz M., Goyke E., Swierczynski J., Rutkowski B., *Metabolism*, **53**, 1060—1065 (2004).
28) Harada T., Kim D. W., Sagawa K., Suzuki T., Takahashi K., Saito I., Matsuura Y., Miyamura T., *J. Gen. Virol.*, **76**, 1215—1221 (1995).
29) Sato S., Fukasawa M., Yamakawa Y., Natsume T., Suzuki T., Shoji I., Aizaki H., Miyamura T., Nishijima M., *J. Biochem.* (Toyko), **139**, 921—930 (2006).
30) Bligh E. G., Dyer W. J., *Can. J. Biochem. Physiol.*, **37**, 911—917 (1959).
31) Nakanishi S., Numa S., *Eur. J. Biochem.*, **16**, 161—173 (1970).
32) Hsu R. Y., Wasson G., Porter J. W., *J. Biol. Chem.*, **240**, 3736—3746 (1965).
33) Ruggieri A., Harada T., Matsuura Y., Miyamura T., *Virology*, **229**, 68—76 (1997).
34) Shi Y., Burn P., *Nat. Rev. Drug Discov.*, **3**, 695—710 (2004).
35) Kim D. W., Suzuki R., Harada T., Saito I., Miyamura T., *Jpn. J. Med. Sci. Biol.*, **47**, 211—220 (1994).
36) Ray R. B., Steele R., Meyer K., Ray R., *J. Biol. Chem.*, **272**, 10983—10986 (1997).
37) Shrivastava A., Manna S. K., Ray R., Aggarwal B. B., *J. Virol.*, **72**, 9722—9728 (1998).
38) Liu P., Ying Y., Zhao Y., Mundy D. I., Zhu M., Anderson R. G., *J. Biol. Chem.*, **279**, 3787—3792 (2004).
39) Kim K. H., *Annu. Rev. Nutr.*, **17**, 77—99 (1997).

All-*trans* retinoic acid down-regulates human albumin gene expression through the induction of C/EBPβ-LIP

Takahiro MASAKI*†‡, Tomokazu MATSUURA§, Kiyoshi OHKAWA†, Tatsuo MIYAMURA*, Isao OKAZAKI‡, Tetsu WATANABE‡ and Tetsuro SUZUKI*[1]

*Department of Virology II, National Institute of Infectious Diseases, Tokyo 162-8640, Japan, †Department of Biochemistry, The Jikei University School of Medicine, Tokyo 105-8461, Japan, ‡Department of Community Health, Tokai University School of Medicine, Kanagawa 259-1193, Japan, and §Department of Laboratory Medicine, The Jikei University School of Medicine, Tokyo 105-8461, Japan

ATRA (all-*trans* retinoic acid), which is a major bioactive metabolite of vitamin A and a potent regulator of development and differentiation, mediates down-regulation of the human albumin gene. However, the mechanism of ATRA-mediated down-regulation is not well understood. In the present study, deletion analysis and luciferase assays demonstrate that ATRA causes a marked decrease in the activity of the albumin promoter, the region between nt -367 and -167 from the transcription start site, where C/EBP (CCAAT/enhancer-binding protein)-binding sites are tightly packed, is indispensable for ATRA-mediated down-regulation. ChIP (chromatin immunoprecipitation) assays revealed that *in vivo* binding of C/EBPα to the region markedly decreases upon incubation with ATRA, whereas ATRA treatment marginally increases the recruitment of C/EBPβ. We found that ATRA has the ability to differentially and directly induce expression of a truncated isoform of C/EBPβ, which is an LIP (liver-enriched transcriptional inhibitory protein) that lacks a transactivation domain, and to increase the binding activity of C/EBPβ-LIP to its response element. Overexpression of C/EBPβ-LIP negatively regulates the endogenous expression of albumin, as well as the activity of the albumin promoter induced by C/EBP transactivators such as C/EBPα and full-length C/EBPβ. In conclusion, we propose a novel model for down-regulation of the albumin gene, in which ATRA triggers an increase in the translation of C/EBPβ-LIP that antagonizes C/EBP transactivators by interacting with their binding sites in the albumin promoter.

Key words: all-*trans* retinoic acid (ATRA), liver-enriched transcription factor, CCAAT/enhancer-binding protein (C/EBP), dominant-negative factor, FLC-4 cell, liver-enriched transcriptional inhibitory protein (LIP).

INTRODUCTION

Serum albumin is the most abundant and characteristic protein that is produced by the mature liver; albumin functions as a transporter of various substances and is a prime regulator of colloid osmotic pressure [1]. Albumin is exclusively synthesized in the liver, approx. 200 mg/kg per day [2], leading to its high steady-state concentration in plasma (35–50 g/l in humans). It has been reported that the albumin level in plasma is decreased as a result of reduced albumin synthesis in clinical disorders such as liver disease [2], infectious disease [3], and cancer [4]. Serum albumin can be used as a reliable indicator for the prognosis and severity of these diseases [5,6]. Therefore it is probable that albumin synthesis is regulated accurately and dramatically in a variety of physiological and pathophysiological conditions.

Albumin synthesis is regulated mainly at the transcriptional level through tissue-specific transcription factors such as HNF (hepatocyte nuclear factor)-1 and C/EBP (CCAAT/enhancer-binding protein) [7,8]. The transcription of the albumin gene is down-regulated by a number of factors, including cytokines [9–11], vitamins [12–14], colloid osmotic pressure [15,16] and amino acid limitation [17]. ATRA (all-*trans* retinoic acid), a major bioactive metabolite of vitamin A, plays a crucial role in hepatocyte differentiation, proliferation and apoptosis [18,19]. ATRA has been shown to down-regulate albumin gene expression in rat hepatocytes [20] and human hepatoma cell lines [12,13]. In animal experiments, it has been reported that a decrease in serum albumin concentration is observed after the administration of ATRA to rodents [21]. Furthermore, in clinical studies of fenretinide (4-hydroxyphenyl-retinamide), a synthetic derivative of ATRA that posesses inhibitory activity against various types of malignant cells [22–24], administration of the drug caused hypoalbuminemia as an adverse effect [25]. Nevertheless, little is known about the ATRA-mediated down-regulation of albumin expression either in experimental or clinical research fields.

In the present study, we have examined the molecular mechanism by which ATRA down-regulates albumin expression in human HCC (hepatocellular carcinoma) cells, with special attention to the transcription factors involved. We present evidence that ATRA preferentially induces the expression of a truncated isoform of C/EBPβ: 20 kDa LIP (liver-enriched transcriptional inhibitory protein). We also present evidence that C/EBPβ-LIP functions as an antagonist of C/EBP transactivators in the expression of the albumin gene.

EXPERIMENTAL

Plasmids

The promoter fragment of the human albumin gene between nt -1867 and $+39$ was obtained by PCR amplification using the genomic DNA of human HCC FLC-4 cells [26,27] as a

Abbreviations used: ATRA, all-*trans* retinoic acid; C/EBP, CCAAT/enhancer-binding protein; C/EBPβ-FL, C/EBPβ-full-length; ChIP, chromatin immunoprecipitation; CUG-BP1, CUG triplet-repeat binding protein 1, DR, direct repeat; eIF, eukaryotic translation initiation factor; EMSA, electrophoretic mobility-shift assay; HCC, hepatocellular carcinoma; HNF, hepatocyte nuclear factor; LAP, liver-enriched transcriptional activator protein; LIP, liver-enriched transcriptional inhibitory protein; RARE, retinoic acid response element; RT, reverse transcriptase.

[1] To whom correspondence should be addressed (email tesuzuki@nih.go.jp).

template; the forward primer (5′-GGCTAGCCTGGACTAATATTATTCTTTTCATTTG-3′) and the reverse primer (5′-CCTCGAGGTGTGCCAAAGGCGTGTGGGGTT-3′) contain restriction sites for NheI and XhoI respectively at the 5′ end. After PCR amplification, the 1.9 kb product was digested with NheI and XhoI and it was then ligated into the pGL3-Basic vector (Promega, Madison, WI, U.S.A.) to produce pAL1.9-LUC. A series of human albumin promoter 5′end-deletion constructs were created by PCR amplification using the above reverse primer and the following forward primers: 1456 bp construct (nt −1417 to +39), 5′-GGCTAGCCAGTACCCATTTCTGAAGAAG-3′; 806 bp construct (nt −767 to +39), 5′-GGCTAGCCCTCATTTGGGTCCATTTTCC-3′; 606 bp construct (nt −567 to +39), 5′-GGCTAGCCAGCTTTTTCAGACAGAATGG-3′; 406 bp construct (nt −367 to +39), 5′-GGCTAGCCTATTTAGTTTGGTTAGTAAT-3′ and 206 bp construct (nt −167 to +39), 5′-GGCTAGCCCAGATGGTAAATATACACAA-3′. Each NheI/XhoI fragment was inserted into the pGL3-Basic vector, to yield pAL1.4-LUC, pAL0.8-LUC, pAL0.6-LUC, pAL0.4-LUC or pAL0.2-LUC. To create expression plasmids for C/EBPα, C/EBPβ-FL (C/EBPβ-full-length) and C/EBPβ-LIP, the corresponding sequences were amplified by PCR using pCMV-C/EBPα and pCMV-C/EBPβ, which were provided by Dr G. J. Darlington (Department of Pathology, Baylor College of Medicine, Houston, TX, U.S.A.), as templates and primers containing an EcoRI site at the 5′ ends. Each EcoRI fragment was cloned into the EcoRI site of the pCAGGS vector [28].

Cell culture and treatment with ATRA

FLC-4 cells were maintained in ASF104 serum-free medium (Ajinomoto, Tokyo, Japan) without any supplements, at 37 °C in a humidified 5 % CO_2/95 % air atmosphere. In experiments using ATRA, FLC-4 cells were cultured in ASF104 serum-free medium with or without 1–1000 nmol/l ATRA (Sigma, St. Louis, MO, U.S.A.). For transient transfection experiments, FLC-4 cells were cultured in Dulbecco's modified Eagle's medium supplemented with 100 units/ml penicillin, 100 μg/ml streptomycin and 10 % foetal bovine serum.

ELISA

Albumin levels in culture medium were measured using a human albumin ELISA quantification kit (Bethyl Laboratories, Montgomery, TX, U.S.A.) according to the manufacturer's instructions.

RNA isolation and real-time RT (reverse transcriptase)-PCR

Total RNA was extracted from FLC-4 cells using the RNeasy mini kit (QIAGEN, Tokyo, Japan) according to the manufacture's protocol. Quantitative real-time RT-PCR analysis was performed using the ABI Prism 7700 Sequence Detector (PerkinElmer Applied Biosystems, Foster City, CA, U.S.A.) as described previously [29]. The standard curve was created using serially diluted total RNA obtained from FLC-4 cultures. The amount of target gene expression was calculated from the standard curve, and its quantitative normalization in each sample was carried out using β-actin (PerkinElmer Applied Biosystems) as an internal control. The following primers and fluorescent dual-labelled probes were used: albumin forward primer, 5′-CGATTTTCTTTTAGGGCAGTAGC-3′; albumin reverse primer, 5′-TGGAAACTTCTGCAAACTCAGC-3′; albumin probe, 5′-CGCCTGAGCCAGAGATTTCCCA-3′; HNF-1α forward primer, 5′-AGCGGGAGGTGGTCGATAC-3′; HNF-1α reverse primer, 5′-CATGGGAGTGCCCTTGTTG-3′; HNF-1α probe, 5′-TCAACCAGTCCCACCTGTCCCAACA-3′; HNF-1β forward primer, 5′-AGCCCAGTTTCCCTTCTATGC-3′; HNF-1β reverse primer, 5′-TCCTCTTCGGTGGTTCCTTGT-3′; HNF-1β probe, 5′-CACAATGCCTCTCCCACGATGTCAAG-3′; C/EBPα forward primer, 5′-CAACGTGGAGACGCAGCA-3′; C/EBPα reverse primer, 5′-GCTCAGCTGTTCCACCCG-3′; C/EBPα probe, 5′-CTGACCAGTGACAATGACCGCCTGC-3′; C/EBPβ forward primer, 5′-GCCCTCGCAGGTCAAGAG-3′; C/EBPβ reverse primer, 5′-TGCGCACGGCGATGT-3′ and C/EBPβ probe, 5′-CAAGCACAGCGACGAGTACAAGATCCG-3′.

Plasmid transfection and luciferase assay

For the expression of luciferase reporter plasmids in FLC-4 cells, 1×10^5 cells per 22 mm well were seeded and cultured overnight. The adherent cells were transfected with 5 μg of plasmid DNA using TransIT-LT1 transfection reagent (Mirus, Madison, WI, U.S.A.) according to the manufacturer's instructions. After the transfection, the cells were incubated with the fresh medium in the presence or absence of 100 nmol/l ATRA for 48 h, followed by determination of the luciferase activity in cells by using the Dual-Luciferase Reporter Assay System (Promega) according to the manufacturer's instructions. For co-expression with C/EBPs, FLC-4 cells were seeded at 2×10^5 cells per 22 mm well on the day before transfection. The cells were transfected with C/EBP expression vectors and the luciferase reporter, pAL1.9-LUC, using TransIT-LT1 transfection reagent, and were cultured for an additional 48 h before the luciferase assay. The total amount of transfected DNA was kept constant by the addition of an empty vector. The pRL-CMV vector (Promega) was used as an internal control for the luciferase assay. To examine the effect of C/EBPs on endogenous albumin expression, FLC-4 cells were seeded at 2×10^5 cells per 22 mm well and cultured overnight. The adherent cells were transfected with C/EBP expression vectors and/or an empty vector using TransIT-LT1 transfection reagent. One day later, the culture medium was changed and the cells were incubated for a further 48 h. After harvesting the medium, the amount of secreted albumin was measured by ELISA.

Western blotting

The proteins were transferred on to a PVDF membrane (Immobilon; Millipore, Bedford, MA, U.S.A.) after separation by SDS/PAGE (12.5 or 15 % gels). After blocking, the membrane was probed with a rabbit polyclonal anti-C/EBPα antibody (sc-61; Santa Cruz Biotechnology, Santa Cruz, CA, U.S.A.), a rabbit polyclonal anti-C/EBPβ antibody (sc-150; Santa Cruz Biotechnology), or a mouse monoclonal anti-β-actin antibody (Sigma), followed by incubation with a peroxidase-conjugated secondary antibody and visualization with a SuperSignal West Pico Chemiluminescent Substrate (Pierce Biotechnology, Rockford, IL, U.S.A.). The amount of protein signal was quantified by densitometric analysis (Cool Saver AE-6955; ATTO, Tokyo, Japan).

ChIP (chromatin immunoprecipitation) assay

ChIP assays were performed using the protocol for the ChIP assay kit (Upstate, Lake Placid, NY, U.S.A.). Briefly, FLC-4 cells in 100 mm dishes were grown to 70 % confluency with or without ATRA treatment for 48 h. The chromatin from formaldehyde-fixed FLC-4 cells was sonicated and immunoprecipitated using the rabbit polyclonal anti-C/EBPα or anti-C/EBPβ antibodies. The chromatin immunoprecipitate was analysed by PCR (33 cycles) with the following primer pairs (F1/R1 and F2/R2) for two different regions of the albumin gene: the region from nt −414

to −188 containing four potential binding sites for C/EBP, F1 (5′-GCAATTTGGGACTTAACTCTTTCAGTA-3′) and R1 (5′-CCTTGTCAATGTATTAAAGTTGTGTAAAACA-3′); and the region from nt −876 to −638 without binding sites for C/EBP, F2 (5′-CAGGGATGGAAAGAATCCTATGCC-3′) and R2 (5′-CCATGTTCCCATTCCTGCTGT-3′).

EMSA (electrophoretic mobility-shift assay)

Nuclear proteins were extracted from FLC-4 cells that were treated with or without 100 nmol/l ATRA for 48 h, or that transiently expressed the LIP protein, using NE-PER Nuclear and Cytoplasmic Extraction reagents (Pierce Biotechnology). A LightShift Chemiluminescent EMSA kit (Pierce Biotechnology) was used to verify the DNA binding of C/EBPβ-LIP to potential C/EBP-responsive sequences in the region from nt −414 to −188 of the albumin gene. Nuclear protein (4 μg) was incubated with the double-stranded biotinylated oligonucleotide that contained the C/EBP-binding site (5′-GTAAAATTTGATAAGATGTT-3′) for 20 min at room temperature. For competition or supershift assay, a 50-fold molar excess of unlabelled wild-type or mutant oligonucleotides (5′-GTAAAAACTGATACAATGTT-3′), or 1 μg of the monoclonal anti-C/EBPβ antibody (sc-7962 X; Santa Cruz Biotechnology) was incubated with nuclear extracts for 30 min before the addition of labelled oligonucleotides. Reaction mixtures were then separated on a 6% native polyacrylamide gel, and shifted bands that corresponded to protein–DNA complexes were captured by a horse radish peroxidase-based detection system.

Statistical analysis

Student's t test was used to evaluate the statistical difference between groups. All P values were obtained using a two-tailed statistical analysis, and $P < 0.05$ was considered statistically significant. Results are means ± S.D.

RESULTS

Down-regulation of albumin secretion and gene expression by ATRA

Among the established human HCC cell lines, FLC-4 is known to have relatively well-preserved liver cell functions, such as albumin synthesis, enzyme activity and drug metabolism [26,27]. When FLC-4 cells were incubated in the presence of ATRA for 48 h, the albumin level in the culture medium was significantly decreased in a dose-dependent manner; the inhibitory effect of ATRA at concentrations of 1, 10, 100 and 1000 nmol/l on albumin production was 37.04 ± 3.60%, 50.04 ± 3.27%, 59.96 ± 4.71% and 65.74 ± 0.74% respectively (Figure 1A). After treatment with 1000 nmol/l ATRA, the growth rate of FLC-4 cells was only slightly (approx. 30%) inhibited, and the cells exhibited no morphological changes (results not shown). To address the mechanism of down-regulation of albumin synthesis by ATRA, the mRNA level of albumin in the cells treated with ATRA for 24 h was examined. As shown in Figure 1(B), consistent with the level of the secreted protein, cellular albumin mRNA expression was inhibited significantly and dose-dependently by ATRA. A 61.95% decrease in the albumin mRNA level was observed in the presence of 100 nmol/l ATRA, demonstrating that albumin synthesis is down-regulated by ATRA via a reduction in the level of mRNA, which is presumably caused by a decrease in transcriptional activity of the albumin gene and/or albumin mRNA stability.

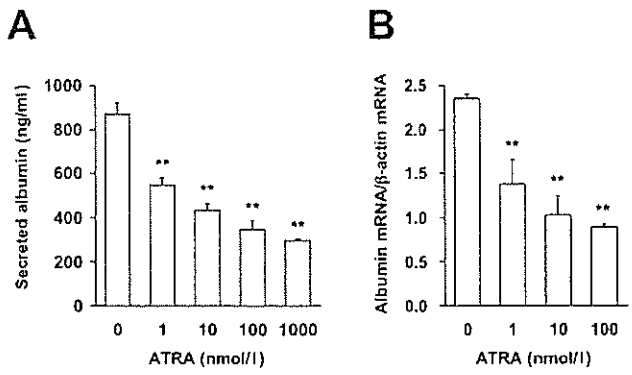

Figure 1 Effect of ATRA treatment on albumin secretion and mRNA expression in FLC-4 cells

(A) The culture medium was collected 48 h after the addition of ATRA. Albumin levels in the medium were quantified by ELISA. $^{**}P < 0.01$ compared with no ATRA treatment. (B) The cells were harvested after incubation with ATRA for 24 h. Albumin mRNA levels were measured by quantitative RT-PCR analysis. Albumin mRNA levels were normalized to β-actin mRNA levels. $^{**}P < 0.01$ compared with control cells without ATRA treatment.

Identification of the 5′ end flanking region of the albumin gene responsible for its transcriptional down-regulation by ATRA

It is well known that the effect of ATRA on the transactivation of target gene expression is mediated by retinoic acid receptors and retinoid X-receptors that bind DNA as a heterodimer [30,31]. These nuclear receptors are ligand-dependent transcription factors that bind RAREs (retinoic acid response elements) consisting of two AGGTCA sites usually arranged as DRs (direct repeats) [30,31]. The RAREs found on ATRA-regulated genes are made up of DR motifs with a spacing of 2 (DR2) or 5 nt (DR5) [31]. However, neither the consensus sequence of RAREs nor RARE-like sequences were identified in the 5′ end flanking region of the human albumin gene by sequence analysis with a computer search program, TFSEARCH (Searching Transcription Factor Binding Sites; http://www.cbrc.jp/research/db/TFSEARCH.html). One can hypothesize that the ATRA-mediated transcriptional regulation of the albumin gene is a secondary response to retinoic acid in human liver cells.

To identify the region responsible for the down-regulation of albumin gene expression by ATRA, a reporter plasmid, pAL1.9-LUC, containing a 1.9 kb fragment of the albumin 5′ end flanking sequence linked to a firefly luciferase gene was constructed (Figure 2B) and transfected into FLC-4 cells. The reporter luciferase assay demonstrated that the activity of the albumin promoter from pAL1.9-LUC was markedly decreased to 30.78% after treatment with ATRA (Figure 2B). This inhibitory effect correlated well with the inhibition of albumin mRNA expression (as shown in Figure 1B), suggesting that the 5′ end 1.9 kb flanking sequence of the albumin gene is involved in transcriptional down-regulation of albumin expression by ATRA. To define an ATRA-responsive element within the 1.9 kb fragment, a series of 5′end-deletion constructs fused with the luciferase gene were created (Figure 2B). As shown in Figure 2(B), deletions that extended to nt −367 (pAL0.4-LUC) resulted in basal promoter activities and an inhibitory effect of ATRA on promoter activity that are comparable with those observed in the cells transfected with pAL1.9-LUC. By contrast, a further deletion up to nt −167, pAL0.2-LUC, yielded a marked decrease in the basal promoter activity, as well as in the inhibitory effect of ATRA on the promoter activity. These results suggest that the region from nt −367 to −167 contains a putative element responsible for

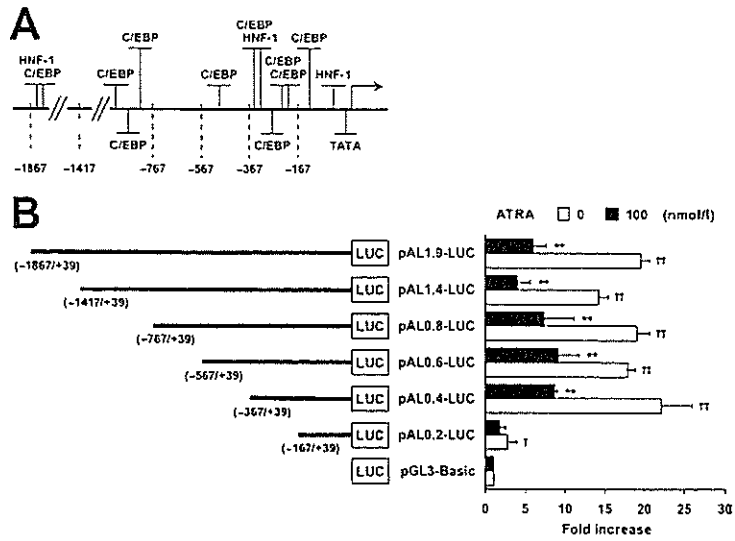

Figure 2 Identification of the 5′ end flanking region of the albumin gene responsible for its transcriptional down-regulation by ATRA

(A) Schematic diagram of the potential binding sites for liver-enriched transcription factors in the 5′ end flanking region of the albumin gene analysed with a computer search program, TFSEARCH. (B) Deletion constructs of the upstream regulatory region of the albumin gene linked to the firefly luciferase reporter gene (LUC) are shown. FLC-4 cells were co-transfected with a *Renilla* luciferase internal control reporter (pRL-CMV) and a firefly luciferase reporter. Then, cells were stimulated with (black columns) or without (white columns) 100 nmol/l ATRA for 48 h. The relative luciferase activity was obtained by normalizing the firefly luciferase activity to the *Renilla* luciferase activity. The value of the empty vector (pGL3-Basic) was set to 1. $^{**}P < 0.01$ compared with transfected cells not exposed to ATRA. $\dagger P < 0.05$; $\dagger\dagger P < 0.01$ compared with cells transfected with empty vector.

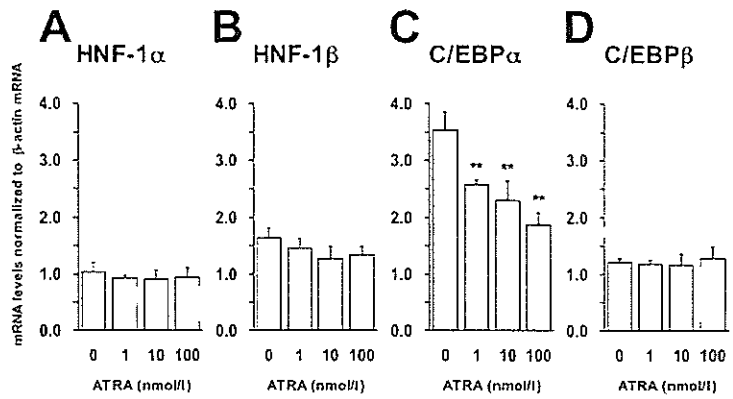

Figure 3 mRNA levels of liver-enriched transcription factors in FLC-4 cells treated with ATRA

The cells were harvested after treatment with ATRA for 24 h, and the mRNA levels of HNF-1α (A), HNF-1β (B), C/EBPα (C) and C/EBPβ (D) were measured by quantitative RT-PCR analysis. The mRNA level of each of these liver-enriched transcription factors was normalized to β-actin mRNA level. $^{**}P < 0.01$ compared with untreated control cells.

transcriptional repression by ATRA and that this region is important for a high level of expression of the human albumin gene.

Effect of ATRA on the expression of transcription factors that possibly bind to the albumin promoter

Several potential *cis*-elements within nt -367 to -167 were identified by sequence analysis using TFSEARCH. This region contained binding sites for liver-specific transcription factors, C/EBPs and HNF-1s, as indicated in Figure 2(A). We next examined whether ATRA regulates expression of these transcription factors at the transcriptional level using quantitative real-time RT-PCR (Figure 3). As shown in Figure 3(C), the mRNA level of C/EBPα, which had the most abundant expression of the four transcription factors tested, was significantly decreased by ATRA treatment in a dose-dependent manner; C/EBPα mRNA expression in FLC-4 cells was suppressed by 47 % in the presence of 100 nmol/l ATRA. By contrast, ATRA exhibited no effect or only a marginal effect on the mRNA levels of HNF-1α, HNF-1β and C/EBPβ (Figure 3A, B and D). Since C/EBPα is known to be a positive regulator of human albumin expression [32,33], it may be possible that down-regulation of C/EBPα expression is one of the mechanisms involved in the inhibitory effect of ATRA on human albumin synthesis.

In vivo recruitment of C/EBPs to the human albumin promoter

To investigate whether the inhibitory effect of ATRA on albumin expression is associated with the recruitment of C/EBPs to

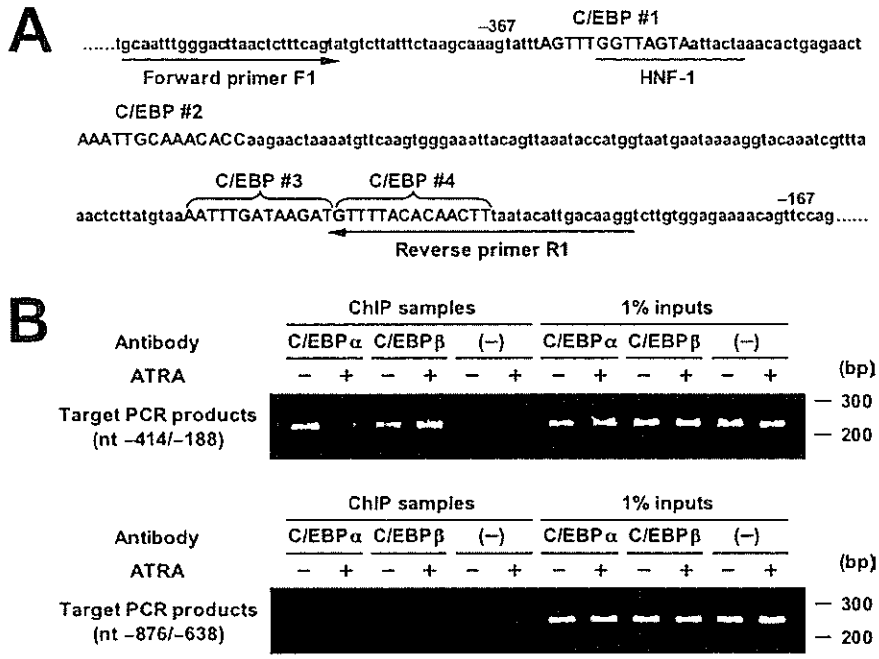

Figure 4 Effects of ATRA on *in vivo* recruitment of C/EBPs to the human albumin promoter

(A) The sequence of the upstream regulatory region (between nt −414 and −188) of human albumin was amplified using a PCR primer pair (F1 and R1), indicated by the arrows. The potential binding sites for C/EBP and HNF-1 in this region are in capital letters and underlined respectively. (B) FLC-4 cells were incubated with or without ATRA (100 nmol/l) for 48 h before the ChIP assay. DNA fragments were amplified with the primers F1 and R1 (upper panel) or F2 and R2 (lower panel). The input represents PCR products from chromatin pellets before immunoprecipitation.

the albumin promoter *in vivo*, we performed ChIP assays of cells treated with or without ATRA (Figure 4). After immunoprecipitation with antibodies against C/EBPα and C/EBPβ, the −414 to −188 nt fragment within the albumin promoter, which contains four potential binding sites for C/EBPs (C/EBP #1–#4 in Figure 4A), was amplified by PCR. The results revealed that under basal conditions both endogenous C/EBPα and C/EBPβ were recruited to the albumin promoter. It is of interest that the *in vivo* binding of C/EBPα to the fragment was markedly decreased upon incubation with ATRA. By contrast, ATRA treatment seemed to marginally increase the recruitment of C/EBPβ to the promoter fragment (Figure 4B). We verified that no DNA fragment was detected in the precipitated chromatin when the region between nt −876 and −638 of the albumin gene, which does not contain binding sites for C/EBP, was amplified by PCR.

These findings suggest that ATRA has the ability to affect the C/EBP occupancy of the albumin promoter *in vivo*. It is possible that impaired C/EBPα binding caused by ATRA leads to down-regulation of albumin gene expression.

ATRA induces expression of C/EBPβ-LIP, and its DNA-binding activity

It has been reported that the gene for C/EBP is transcribed into a single mRNA that encodes several N-terminally truncated protein isoforms, possibly via the process of alternative translation initiation at downstream AUG codons [34,35]. C/EBPα mRNA is translated into two major proteins of 42 and 30 kDa (p42- and p30-C/EBPα) [34,36], whereas C/EBPβ mRNA mainly produces three isoforms referred to as C/EBPβ-FL, LAP (liver-enriched transcriptional activator protein) and LIP, which are 46, 42, and 20 kDa respectively [34,37,38]. All of the C/EBP isoforms have DNA-binding and dimerization domains. However, p30-C/EBPα and LIP are translated from the third in-frame AUG start codon [34,36] and lack most of the transactivation domain [34,37,39]. Although p42-C/EBPα, C/EBPβ-FL and LAP transactivate their target genes' expression, p30-C/EBPα and LIP are unable to activate gene transcription and are able to function as dominant-negative factors by antagonizing and by competing with other C/EBP transactivators [34,37]. It has been considered that the ratio of C/EBP transactivators to C/EBP dominant-negative factors is important in controlling each activity of C/EBPα and C/EBPβ [34,36,37].

We determined the effect of ATRA on the expression of C/EBP isoforms by Western blotting (Figure 5A). An increased level of LIP was observed as early as 8 h after ATRA treatment and it was also detected after 48 h of treatment. By contrast, C/EBPβ-FL and LAP isoforms showed little change in their expression after the 48 h time point of ATRA treatment. The expression level of C/EBPα showed no change in the presence of ATRA after 8 or 16 h. Although a decrease in C/EBPα expression was found after 48 h of ATRA treatment, it is not likely that this reduction is the cause of down-regulation of albumin expression, since a decreased level of albumin mRNA was observed as early as 24 h after ATRA treatment (Figure 1B). It appears that the ratio of LIP to C/EBPβ-FL and LAP was elevated in a dose-dependent manner after 16 h of ATRA treatment, while the ratio of p42-C/EBPα to p30-C/EBPα showed no difference with or without ATRA treatment until 48 h after the addition of ATRA. These results demonstrate that ATRA has the ability to differentially modulate the level of C/EBP isoforms with an increase in LIP and a decrease in C/EBPα; the expression of LIP is induced immediately in response to ATRA treatment.

We next examined the effect of ATRA on the DNA-binding activity of LIP, by EMSA (Figure 5B). The nucleotide sequence of C/EBP-binding site #3, which is present in the region from

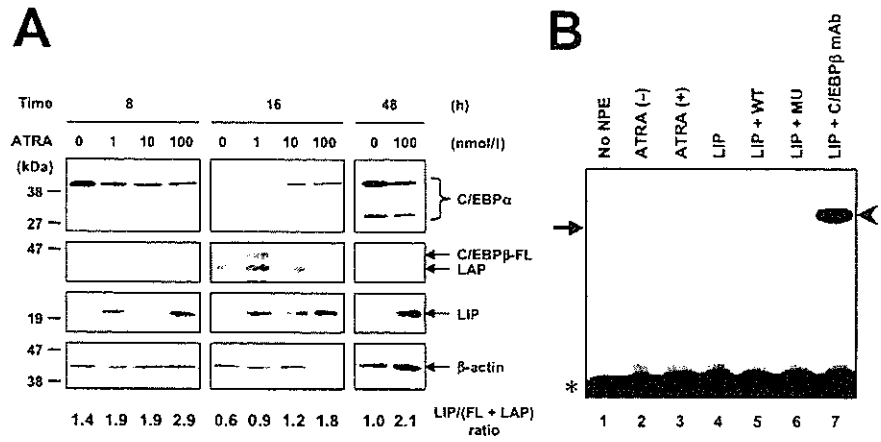

Figure 5 Effect of ATRA on protein expression of C/EBPs, and DNA-binding activity of C/EBPβ-LIP

(**A**) FLC-4 cells were incubated with ATRA (100 nmol/l) for 8, 16 and 48 h. After harvesting, total cellular proteins were resolved by SDS/PAGE, and the presence of C/EBPα and C/EBPβ was analysed by Western blotting. The ratio of C/EBPβ-LIP to C/EBPβ-FL and -LAP [LIP/(FL + LAP)] was measured by densitometric analysis. (**B**) Nuclear proteins were extracted from FLC-4 cells treated with or without 100 nmol/l ATRA for 48 h, or cells that transiently expressed the LIP protein, and were analysed by EMSA as described in the Experimental section. Lane 1, no nuclear protein extracts (NPE); lane 2, FLC-4 cells incubated without ATRA; lane 3, FLC-4 cells incubated with ATRA; lane 4, FLC-4 cells transiently expressing the LIP protein; lane 5, addition of a 50-fold molar excess of unlabelled wild-type (WT) oligonucleotides to the mixture in lane 4; lane 6, addition of a 50-fold molar excess of unlabelled mutant (MU) oligonucleotides to the mixture in lane 4; lane 7, addition of an anti-C/EBPβ monoclonal antibody (mAb) to the mixture in lane 4. The arrow, arrowhead and asterisk indicate a DNA–LIP complex, a DNA–LIP-antibody complex (supershifted band) and a free probe respectively.

nt −367 to −167 of the albumin gene, as shown in Figure 4(A), was used as a DNA probe. A shifted band, which was observed in FLC-4 cells that transiently express LIP protein (Figure 5, lane 4), was removed by the addition of an excess of unlabelled homologous probe (lane 5), but not by the addition of a mutated sequence (lane 6). This band was supershifted by the addition of the C/EBPβ antibody (lane 7). The results indicate that LIP binds to its binding motif within the albumin promoter.

In the presence of ATRA (Figure 5, lane 3), a shifted band that corresponded to endogenous LIP-bound DNA was observed, which was more intense than in the absence of ATRA (lane 2). We also confirmed that endogenous LIP bound to the other three binding sites for C/EBP (#1, #2 and #4) (results not shown). Thus the combined data demonstrate that ATRA induces not only the expression of LIP but also its DNA-binding activity.

C/EBPβ-LIP down-regulates the gene expression and synthesis of albumin by blocking the transcriptional activity of C/EBPα and C/EBPβ-FL

Our data suggest that early induction of LIP expression and an increase in the DNA-binding activity of LIP caused by ATRA triggers the down-regulation of albumin gene expression. To directly evaluate the role of LIP in albumin expression, we determined the effect of C/EBPs on albumin expression using transient transfection experiments (Figure 6). As shown in Figure 6(A), overexpression of C/EBPα and C/EBPβ-FL caused a more than 20.7- or 8-fold increase respectively, in promoter activity in a dose-dependent manner compared with transfection with an empty vector. By contrast, co-expression with LIP resulted in a marked and dose-dependent reduction of the increased activity (Figure 6B). Expression of LIP alone also decreased the level of promoter activity (Figure 6B), presumably because LIP inhibited positive functions of endogenous C/EBP transactivators expressed in FLC-4 cells. We investigated the effect of C/EBP expression on the secretion of endogenous albumin (Figure 6C). Consistent with albumin promoter activity, overexpression of C/EBPα and C/EBPβ-FL significantly increased the level of albumin in the culture mediun by 2- and 1.7-fold respectively, compared with transfection with an empty vector. Overexpression of LIP significantly and dose-dependently decreased both the basal level of albumin secretion and the level of albumin elevated by expression of C/EBPα and C/EBPβ-FL. Thus these results strongly suggest that LIP plays a role in repressing albumin gene expression by blocking the ability of C/EBP transactivators to activate the albumin promoter, leading to down-regulation of albumin synthesis.

DISCUSSION

In the present study, we have demonstrated the down-regulation of secretion and gene expression of albumin mediated by ATRA. This finding is in line with previous reports that ATRA negatively regulates albumin synthesis in rat hepatocytes [20] and human hepatoma cell lines [12,13]. We addressed its molecular mechanisms and found: (i) that the 5′ end flanking region of the albumin gene, nt −367 to −167, in which four binding sites for C/EBPs are conserved, is responsible for its transcriptional repression by ATRA, and (ii) that upon ATRA treatment, C/EBPβ-LIP is differentially induced among C/EBPβ isoforms and the expression of C/EBPα is subsequently decreased. The present study reveals that C/EBP proteins play a key role in the transcriptional regulation of the human albumin gene by ATRA.

C/EBPα and C/EBPβ, which are composed of DNA-binding and dimerization domains at their C-termini, and transactivation domains at their N-terminal regions, are expressed in the liver at high levels and are involved in the regulation of cell growth, cell differentiation, metabolism and inflammation [40–42]. A single mRNA species for C/EBPβ directs production of three major isoforms in liver tissues: C/EBPβ-FL, LAP and a low-molecular-mass isoform, LIP [34,37,38]. These three proteins contain the DNA-binding and dimerization domains. C/EBPβ-FL and LAP contain a transactivation domain and function as transcriptional activators, whereas LIP lacks the N-terminal transactivation domain and can attenuate the transcriptional stimulation by

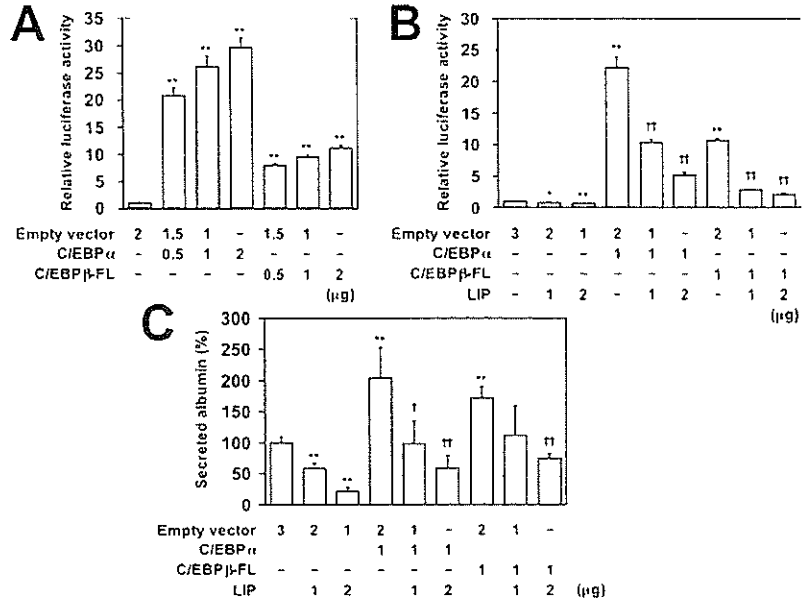

Figure 6 C/EBPβ-LIP down-regulates the promoter activity and synthesis of albumin by blocking C/EBP transcriptional activity

(**A**) and (**B**) FLC-4 cells were transfected with pAL1.9-LUC and pRL-CMV in the presence or absence of C/EBP expression vectors. After incubation for 48 h, the cells were harvested and assayed for luciferase activity. The relative luciferase activity was obtained by normalizing the pAL1.9-LUC activity to the pRL-CMV activity, and the value of the empty vector (pCAGGS) was set to 1. $*P < 0.05$; $**P < 0.01$ compared with cells transfected with empty vector. $††P < 0.01$ compared with cells expressing C/EBPα or C/EBPβ-FL alone. (**C**) FLC-4 cells were transfected with C/EBP expression vectors and/or an empty vector. After 72 h, the medium was harvested, and the amount of secreted albumin was quantified by ELISA. The value of the empty vector was set to 100%. $**P < 0.01$ compared with transfection with empty vector. $†P < 0.05$; $††P < 0.01$ compared with cultures that express C/EBPα or C/EBPβ-FL alone.

C/EBPβ-FL, LAP and C/EBPα in substoichiometric amounts [37]. It has been shown that LIP is involved in the down-regulation of human *CYP3A4* induced by interleukin-6 [43] and in the repression of C/EBPα mRNA during the acute phase of the immune response [44]. In the present study, we have demonstrated that the overexpression of LIP leads to inhibition of the positive regulation of albumin promoter activity that is mediated by C/EBPα and C/EBPβ-FL (Figure 6B). This is the first study to show the involvement of LIP in the regulation of human albumin gene expression.

Our albumin promoter assay using the 5′end-deletion constructs demonstrated that the region spanning nt −367 to −167 within the albumin gene is a prerequisite for ATRA-dependent transcriptional down-regulation (Figure 2B). The ChIP assay showed that during ATRA treatment the *in vivo* binding of C/EBPα to the region clearly decreased, whereas the binding of C/EBPβ slightly increased (Figure 4B). The anti-C/EBPβ antibody used in the present study is capable of recognizing all of the C/EBPβ isoforms, since no anti-C/EBPβ antibodies that recognize the N-termini of C/EBPβ are available to distinguish these isoforms. However, an EMSA demonstrated that ATRA increased the binding activity of LIP to its response element in this region (Figure 5B). Thus we suggest that the increase in DNA-binding of C/EBPβ, as shown in the ChIP assay, is caused by ATRA-induced LIP expression. It has been reported that LIP has a greater binding capacity for the C/EBP-binding element compared with C/EBP transactivators i.e. LIP binds to the element 4-fold more efficiently than does LAP [37]. Therefore it is probable that C/EBP transactivators predominantly bind to their response elements within the albumin promoter in the ATRA-untreated cells, while an increased level of LIP possibly displaces these transactivators at the C/EBP-binding sites to occuy them in ATRA-treated cells.

As indicated in Figure 5(A), preferential induction of LIP expression by ATRA was observed even in the culture after

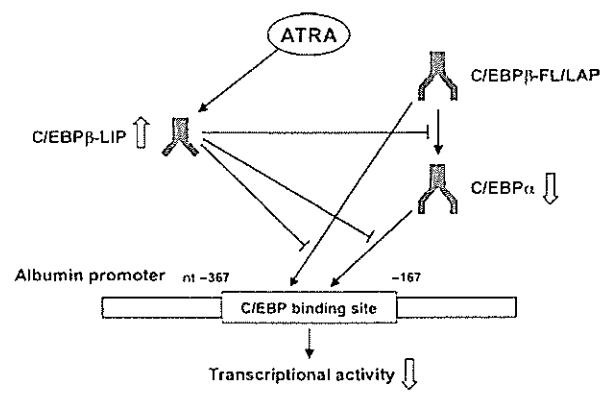

Figure 7 Proposed mechanism by which ATRA down-regulates albumin gene transcription in FLC-4 cells

An ATRA signal increases the expression of C/EBPβ-LIP in FLC-4 cells. This truncated C/EBP protein directly and indirectly down-regulates the expression of the albumin gene by competing with C/EBP transactivators and inhibiting C/EBPα expression.

8 h of ATRA treatment. By contrast, a decrease in C/EBPα gene expression was not detected at such an early stage (results not shown), but was first observed 24 h after the addition of ATRA (Figure 3C). Furthermore, the expression level of C/EBPα protein was little changed when the mRNA expression level of albumin was decreased by ATRA treatment (Figure 5A). Based on the results of the present study, we propose a model for the molecular mechanism by which ATRA down-regulates the expression of human albumin in liver-derived cells (Figure 7). ATRA triggers the differential induction of C/EBPβ-LIP, a dominant-negative regulator of C/EBP activators. A C/EBP-binding consensus sequence has been identified in the C/EBPα